Helsinki University of Technology Laboratory of Space Technology
Espoo, 2006 REPORT 66

# MICROWAVE MODELS OF SNOW CHARACTERISTICS FOR REMOTE SENSING

**Ali Nadir Arslan**

**Dissertation for the degree of Doctor of Science in Technology to be presented with due permission of the Department of Electrical and Communications Engineering for public examination and debate in Auditorium S4 at Helsinki University of Technology (Espoo, Finland) on the 4th of December, 2006, at 12 o'clock noon.**

**Helsinki University of Technology**
**Department of Electrical and Communications Engineering**
**Laboratory of Space Technology**

**Teknillinen korkeakoulu**
**Sähkö- ja tietoliikennetekniikan osasto**
**Avaruustekniikan laboratorio**

Helsinki University of Technology

Mailing address:
Laboratory of Space Technology
P.O.Box 3000
FIN-02015 TKK
Finland

Street address:
Otakaari 5 A
FIN-02150 Espoo

Tel. +358 9 451 2378
Fax +358 9 451 2898

ISBN 13 978-951-22-8531-0 (printed)
ISBN 10 951-22-8531-2 (printed)
ISBN 13 978-951-22-8532-7 (electronic)
ISBN 10 951-22-8532-0 (electronic)
ISSN 0786-8154

Picaset Oy
Helsinki 2006

# Table of Contents

# Preface

This thesis has been conducted in the Laboratory of Space Technology in Helsinki University of Technology under the supervision of Prof.Dr. Martti Hallikainen.

I would like to express my gratitude to Prof.Dr. Martti Hallikainen for acting as the supervisor and the tutor in all of the papers and in my thesis. I also would like to thank the whole personnel of the Laboratory of Space Technology, especially Kimmo Rautiainen, Jaan Praks, Simo Tauriainen, Sampsa Koponen, Pekka Ahola, Irja Kurki and Irma Planman for creating a very friendly working environment. Furthermore I want to thank Dr. Jarkko Koskinen and Dr. Jouni Pulliainen for helping and guiding my research by spending their valuable time in discussions with me. I would also like to thank Wang Huining first of all for being a good friend, and secondly for having very valuable scientific discussions and finally being co-author in my papers. I would like to thank also Prof.Dr. Ari Sihvola, Prof.Dr. Keijo Nikoskinen and Prof.Dr. Kirsi Virrantaus for valuable discussions and lectures.

I would like to thank all my friends in Finland, especially Auni Pajari and her family (Tapsa, Matias, Carolus, Nelli and Milla), Arzu Coltekin, Cumhur Erkut and his family (Anu and their beautiful daughter), Csilla Bors and her family (Jari and Noora), Gulistan Anul and her family (Pasi and Yasemin), Zekeriya Uykan, Ilke Senol and his family (Kati and Emre), Hakan Cuzdan, Burcu and Cem Ecevitoglu and their new born son, Oguz and Arzu Tanzer, Yonca, Murat and Ballihan Ermutlu, Asli Tokgöz and her family, Jafar Keshvari and his family, Haydar Aydin, Engin Köseoglu and his family, Kimmo Sairanen, Susanna Hart, and Katja Sorvali, Matti Perä-Rouhu, Kerttu Suomalainen, Laszlo Sule and Turkish Folk Dance group, HOT, members (especially Mustafa, Leena, Mirja, Leo and Riitta) for being part of my life. I would like to thank Nokia Research Center for supporting my studies by creating a flexible working environment especially Olli Salmela, Ilkka Kelander, Ville Hurskainen, Jukka Rantala, Tapani Ryhänen and Hannu Kauppinen.

Finally, I am also very grateful to all of my family members and my friends in Turkey for loving me always.

# Abstract

One of the key problems of microwave remote sensing is the development of theoretical microwave models for terrain such as soil, vegetation, snow, forest, etc., due to the complexity of modeling of microwave interaction with the terrain. In this thesis this problem is approached from the new point of view of both empirical models and rigorous theoretical models. New information concerning radar remote sensing of snow-covered terrain and permittivity of snow has been produced. A C-band semi-empirical backscattering model is presented for the forest-snow-ground system.

The effective permittivity of random media such as snow, vegetation canopy, soil, etc., describes microwave propagation and attenuation in the media and is a very important parameter in modeling of microwave interaction with the terrain. Good permittivity models are needed in microwave emission and scattering models of terrain. In this thesis, the strong fluctuation theory is applied to calculate the effective permittivity of wet snow. Numerical results for the effective permittivity of wet snow are illustrated. The results are compared with the semi-empirical and the theoretical models. A comparison with experimental data at 6, 18 and 37 GHz is also presented. The results indicate that the model presented in this work gives reasonably good accuracy for calculating the effective permittivity of wet snow. Microwave emission and scattering theoretical models of wet snow are developed based on the radiative transfer and strong fluctuation theory. It is shown that the models agree with the experimental data.



**Keywords:** Remote sensing, radar, radiometer, correlation functions, effective permittivity, snow, dry snow, wet snow, radiative transfer theory, strong fluctuation theory, microwave emission modeling, microwave scattering modeling, backscattering.

## List of Appended Papers

This thesis is based on the work contained in the following papers,

[**P1**] Arslan, A.N., Praks, J., Koskinen, J. and Hallikainen, M., "An empirical model for retrieving of snow water equivalent from C-band polarimetric SAR data," *Report No. 45, Laboratory of Space Technology, Helsinki University of Technology*, Espoo ISSN 0786-8154, ISBN 951-22-5406-9, 2001.

[**P2**] Arslan, A.N., Pulliainen, J. and Hallikainen, M., "Observation of L- and C-band backscatter and a semi-empirical backscattering model approach from a forest-snow-ground system," *Progress in Electromagnetics Research, PIER 56*, pp. 263-281, 2006

[**P3**] Arslan, A.N., Huining, W., Pulliainen, J. and Hallikainen, M., "Effective permittivity of wet snow by strong fluctuation theory, " *Journal of Electromagnetic Waves and Applications*, Vol.15, pp. 53-55 (abstract), *Progress in Electromagnetics Research, PIER 31*, pp. 279-296 (the complete text), 2001.

[**P4**] Huining, W., Arslan, A.N., Pulliainen, J. and Hallikainen, M., "Microwave emission model for wet snow by using radiative transfer and strong fluctuation theory," *Journal of Electromagnetic Waves and Applications*, Vol.15, pp. 57-59 (abstract), *Progress in Electromagnetics Research, PIER 31*, pp. 297-316 (the complete text), 2001.

[**P5**] Arslan, A.N., Huining, W., Pulliainen, J. and Hallikainen, M., " Scattering from wet snow by applying strong fluctuation theory," *Journal of Electromagnetic Waves and Applications*, Vol.17, 1009-1024, 2003.

[**P6**] Arslan, A.N., Hallikainen, M., Pulliainen, J., "Investigating of snow wetness parameter using a two-phase backscattering model," *IEEE Transaction on Geoscience Remote Sensing*, Vol. 43, No. 8, pp. 1827-1833, 2005.

The research work in papers [**P1**], [**P2**], [**P5**], [**P6**] was carried out by the first author alone, with the co-authors acting as scientific advisors. In [**P3**] and [**P4**], the ideas came from close discussions between the first and second author; the other co-authors performed as scientific advisors. In [**P3**], the first author worked with the existing semi-empirical models and three-phase model for effective permittivity of wet snow and compared our new model with those models and experimental data; the second author dealt with the development of the two-phase model by using the strong fluctuation theory. In [**P4**], the first author worked on model development and the second author concentrated on calculating the effective permittivity of wet snow.

# List of Symbols and Abbreviations

| | |
|---|---|
| A | Area |
| B | Brightness |
| $B_{bb}$ | Brightness of a blackbody |
| $C$ | Speed of light in vacuum, 2.9979 x $10^8$ m / s |
| $D$ | Diameter of the scatterer |
| $E$ | Emissivity |
| $F$ | Frequency |
| $f_v$ | Fraction volume |
| $k_B$ | Boltzmann's constant, 1.36 x $10^{-23}$ joule / K |
| $K$ | Wave number, $k = \omega\sqrt{\mu\varepsilon}$ |
| $k_0$ | Wave number in free space, $k_0 = \omega\sqrt{\mu_0\varepsilon_0} = 2\pi / \lambda$ |
| $L$ | Correlation length |
| $l_p$ | Correlation length in horizontal direction |
| $l_z$ | Correlation length in vertical direction |
| $m_v$ | Liquid water content |
| $P$ | Power |
| $R$ | Radius of scatterer |
| $T$ | Temperature |
| $T_B$ | Brightness temperature |
| $\varepsilon$ | Permittivity or dielectric constant |
| $\varepsilon_0$ | Permittivity of free space, 8.854 x $10^{-12}$ F / m |
| $\varepsilon_{eff}$ | Effective permittivity |
| $\lambda$ | Wavelength |
| $\omega$ | Angular frequency, $2\pi f$ |
| $\hbar$ | Planck's constant |
| $\sigma$ | Scattering cross section |

| | |
|---|---|
| ACF | Autocorrelation function |
| CRT | Conventional radiative transfer |
| DMRT | Dense medium radiative transfer |
| EMAC | European multisensor airborne campaign |
| TKK | Helsinki University of Technology, Finland |
| IEM | Integral equation Model |
| KA | Kirchhoff approximation |
| MEMLS | Microwave emission model of layered snowpacks |
| NDVI | Normalized difference vegetation index |
| QCA | Quasi-crystalline approximation |
| RMSE | Root mean square equation |
| SAR | Synthetic aperture radar |
| SPM | Small perturbation method |
| SSA | Small slope approximation |
| SWE | Snow water equivalent |

# I Introduction

In the field of microwave remote sensing the physical phenomena governing the backscattering from the terrain such as snow, forest, soil and etc., is a very complicated problem due to the complex behavior of microwave interaction with the terrain. Microwave sensors such as radiometers and radars are often used for snow and forest studies in microwave remote sensing because of their usability under varying weather conditions. Factors like clouds, rain and lack of light do not affect the measurements. Radiometers are passive sensors that measure the thermal emission radiated by the target. Radars are active sensors that transmit a signal to the target and measure the signal scattered back from the target. Active microwave sensors have proven to be a valuable tool in microwave remote sensing of snow cover (*Stiles and Ulaby 1980, Ulaby and Stiles 1980, Mätzler 1983, Kendra et al. 1998, Shi and Dozier 2000, Koskinen 2001*). Passive microwave sensors have been studied for snow monitoring (*Hallikainen and Jolma 1992, Mätzler 1994, Wiesman et al. 1998, Pulliainen et al. 1999, Macelloni et al. 2005, Markus et al. 2006*). In forest applications, active microwave sensors are mainly used because they have better ground resolution than passive microwave sensors and the intensities of microwave thermal emission from ground are close to those from the forest in most of the cases. Many studies have been conducted concerning the utilization of radar remote sensing for forest applications (*Durden et al. 1989, Dobson et al 1992, Le Toan 1992, Pulliainen 1994, Pulliainen et al 1994, Liang et al. 2005, Askne and Santoro 2005, Du et al. 2006, Izzawati et al. 2006*).

In theoretical microwave modeling of the terrain, calculation of the effective permittivity of a random medium is essential. Investigation of the effective permittivity of snow has a long history. Experimental studies of the effective permittivity of snow started in 1952 (*Cumming 1952*) and were followed by many others (*Glen and Paren 1975, Colbeck 1980, Ambach and Denoth 1980, Tiuri et al. 1984, Mätzler et al. 1984*). A summary of semi-empirical dielectric models of

snow is found in (*Hallikainen et al. 1986*). The strong permittivity fluctuation theory for snow cover was introduced in 1986 (*Stogryn 1986*) and its application to calculate the effective permittivity has been reported by many authors (*Tsang et al. 1982, Yueh and Kong 1990, Lim et al. 1994, Nghiem et al. 1993, and Nghiem et al. 1995*).

Microwave scattering and emission models of snow have been studied by many authors. *Fung* (*1994*) presented a scattering model for a snow layer. Snow layer is modeled as a volume of Mie scatterers (ice particles). The boundaries of the snow layer are modeled using the Integral Equation Model (IEM) (*Fung 1994*). The effects of volume and surface scattering are integrated by applying the matrix doubling method (*Ulaby et al. 1986, Fung 1994*). A polarimetric model that includes both surface and volume scattering as well as the interaction terms between surface and volume has been developed (*Shi and Dozier 1993, Shi and Dozier 1995*). Radiative transfer model for dense media is used for the volume scattering component. The surface scattering model, IEM, is used to evaluate the surface scattering components and introduced to the radiative transfer equations as the boundary conditions in order to evaluate the importance of the interactions between the surface and volume scattering signals.

The strong fluctuation theory has been applied to calculate scattering from snow (*Tsang et al. 1982, Jin and Kong 1984*). *Tsang et al. (2003)* applied quasicrystalline approximation (QCA) dense medium theory to calculate the absorption, scattering and emission of snow at multiple frequencies. A microwave emission model from random medium with non-spherical scatterers was improved by using the radiative transfer equations and the strong fluctuation theory. The model was then applied to describe microwave emission from wet snow (*Huining 2001*).

The objectives of the thesis are

(1) to understand better the relationship between radar signatures and snow,
(2) to develop a semi-empirical model of a snow-forest-ground system,
(3) to study the effective permittivity of wet snow using strong fluctuation theory with non-symmetrical inclusions,
(4) to apply microwave emission and scattering models to retrieve snow parameters such as snow water equivalent and snow wetness.

Chapter 2 introduces the use of active and passive sensors in microwave remote sensing and microwave emission and backscattering models for interpreting microwave interactions from snow-covered terrain.

In Chapter 3 physical and microwave characteristics of snow, forest and soil are given.

Chapter 4 discusses the results of the research conducted in the thesis.

Chapter 5 and 6 present the conclusions from the thesis and summaries of the appended papers.

# II Microwave Remote Sensing of Snow and Forest

## 2.1 Radar and Radiometer Remote Sensing

*In radar remote sensing*, an antenna is used to transmit electromagnetic waves, and to receive the response from the target. Because of its own illumination radar is an active sensor. Radar consists of a transmitter, a receiver, an antenna, and an electronics system. Radar operates in a frequency range of about 300 MHz to 30 GHz. That is why radar signals are not affected by atmospheric conditions such as clouds or rain. The orientation of received or transmitted electric field is called polarization. There can be four different combinations of both transmit and receive polarizations given below:

(1) HH - for horizontal transmit and horizontal receive,

(2) VV - for vertical transmit and vertical receive,

(3) HV - for horizontal transmit and vertical receive, and

(4) VH - for vertical transmit and horizontal receive.

The relation between the transmitted and received electromagnetic signal is

$$\frac{P_r}{P_t} = \sigma \frac{\lambda^2 G^2}{(4\pi)^3 R^4} \tag{2.1.1}$$

where transmitted and received power are denoted by $P_t$ and $P_r$ respectively, and $G$ is antenna gain. R is the distance to the scattering target. $\sigma$ is scattering cross section, which is related to a physical surface that affects the scattering. A normalized scattering cross section per unit surface $\sigma^0 = \sigma / A_g$, where $A_g$ represents the geometric surface of the scattering. Normalized radar cross section is often expressed in decibels (dB). Typical values of $\sigma^0$ for natural surfaces range from +5 dB (very bright) to –40 dB (very dark). The intensity of backscattered signal is dependent on how the radar signal interacts with the surface. This interaction is affected by both radar parameters (frequency, polarization, viewing geometry, etc.) and the characteristics of the surface such as

land type (forest, snow, bare soil) and topography. Main important characteristics of the interaction between radar and target can be listed as follows:

- Surface roughness of the target
- Radar viewing and surface geometry relationship (local slope)
- Moisture content and electrical properties of the target (effective permittivity).

*Passive Remote Sensing* is the measurement of the electromagnetic radiation from the interaction between the atoms and the molecules in the material. In thermodynamic equilibrium, a material absorbs and radiates energy at the same rate. A blackbody is defined as an ideal material that absorbs all of the incident radiation and reflects none. For the radiometer, the radiated source is the target itself. The power emitted by a target in thermodynamic equilibrium is a function of its physical temperature.

The brightness $B$ is defined representing the radiated power per unit solid angle per unit area as (*Ulaby et al. 1981*):

$$B(f) = \frac{\partial^2 P(f)}{\partial \Omega \, \partial A} \tag{2.1.2}$$

where f is frequency and the P is the power that radiates from the area $\partial A$ to the solid angle $\partial \Omega$.

According to Planck's radiation law (*Ulaby et al. 1981*), a blackbody radiates uniformly in all directions with a spectral brightness, $B$:

$$B = \frac{2\hbar f^3}{c^2} \frac{1}{e^{hf/k_B T} - 1} \tag{2.1.3}$$

where $\hbar$ is Planck's constant; f is frequency; c is speed of light; $k_B$=Boltzmann's constant $= 1.38 \times 10^{-23}$ joule $K^{-1}$; T is temperature. The low frequency region of Planck's radiation law is called Rayleigh-Jeans

approximation valid for $hf / k_B T << 1$; its brightness is given by (*Ulaby et al. 1981*):

$$B = \frac{2k_B T}{\lambda^2} \tag{2.1.4}$$

where $\lambda$ is the wavelength. The brightness of a blackbody for a narrow bandwidth $\Delta f$ at a temperature T is then (*Ulaby et al. 1981*):

$$B_{bb} = B \cdot \Delta f = \frac{2k_B T}{\lambda^2} \cdot \Delta f \tag{2.1.5}$$

The brightness of the material relative to that of a blackbody at the same temperature is defined by emissivity (*Ulaby et al. 1981*):

$$e(\theta, \phi) = \frac{B(\theta, \phi)}{B_{bb}} \tag{2.1.6}$$

where $B(\theta, \phi)$ is the brightness of the real material.

The measured brightness is usually expressed as a brightness temperature. The brightness temperature $T_B$ of an object is the product of its emissivity and physical temperature (*Ulaby et al. 1981*):

$$T_B = e(\theta, \phi) T \tag{2.1.7}$$

The brightness of an object in terms its brightness temperature can be rewritten in a form similar to that of a blackbody (*Ulaby et al. 1981*):

$$B(\theta, \phi) = \frac{2k_B T_B}{\lambda^2} \cdot \Delta f \tag{2.1.8}$$

## 2.2 Microwave Backscattering Models for Snow-Covered Terrain

Understanding of the relationship between radar signature and snow is very important for retrieving desired snowpack parameters such as snow density, snow water equivalent and snow wetness which are important in natural sciences, particularly in hydrology and climatology. The backscattered signal measured by the radar is the sum of the contributions from physical interactions in snow and between snow and its surroundings such as air, vegetation canopy, and ground. In order to understand the relationship between backscattering signature and the snow parameters, one should take into account all effects such as instrumental parameters (polarization, frequency, incidence angle) and snow parameters (temperature, size and shape of inclusions, water content of snow, snow thickness, and snow-ground, snow-vegetation, and air-snow interfaces (or surface roughness)). In general, the backscattering signal of snow is the sum of signal contributions from (a) *snow-air interface*, (b) *volume scattering of snow* and (c) *snow-ground interface* (*Ulaby et al. 1986, Fung 1994*).

*Surface scattering models* based on both the Small Perturbation Method (SPM) and the Kirchhoff Approximation (KA) has been widely used in the past in the theoretical modeling of microwave remote sensing (*Ulaby et al. 1982, Tsang et al. 1985, Fung 1994, Tsang and Kong 2001*). Other recent surface scattering models such as the Integral Equation Model (IEM) (Fung et al. 1992, Fung 1994) and the Small Slope Approximation (SSA) have shown great promise in the prediction of surface scattering (*Voronovich 1994, Irisov 1997*).

SPM is valid for slightly rough surfaces, while KA is applicable for a rough surface with a large surface curvature. The results for emissivity are the same for SSA and SPM. IEM is in agreement with SPM for slightly rough surface and with KA in the range of KA holding. The Integral Equation Model (IEM) with a transitional function (Wu et al. 2001) can provide very well backscattering coefficients for a wide range of surface roughness parameters. The idea behind introduction of a transition function in the calculation of Fresnel reflection

coefficients is to take spatial dependence into account and thus removed the restrictions on the limits of surface roughness permittivity. SPM and SSA can lead to erroneous results for emissivities of rough surfaces with moderate root mean-square (rms) slopes.

Development of a surface scattering model called Advanced IEM (AIEM) by extending the existing integral-equation-based surface scattering model (IEM) has led to a more accurate calculation of a single scattering for a surface with a large rms slope (Chen et al. 2003).

*In modeling of volume scattering from snow* the scatterers are assumed to be randomly oriented and they are replaced by spheres. The simplification of the problem is done by using the effective size of scatterers instead of their size distribution. These modeling approximations have shown satisfactory predictions (*Fung and Eom 1985, Tjuatja et al. 1992, 1993*). Other modeling approaches using a strong fluctuation theory and a size distribution in the radiative transfer theory for snow have been considered (*Stogryn 1985, Stogryn 1986, Nghiem 1993, Wen et al. 1990*).

*Fung* (*1994*) presented a scattering model for a snow layer. Snow layer is modeled as a volume of Mie scatterers (ice particles). The Mie solution of the field scattered from a sphere utilized to derive the volume scattering phase matrix for a closely packed medium. The boundaries of the snow layer are modeled using the surface scattering model, IEM (*Fung 1994*). The effects of volume and surface scattering are integrated by applying the matrix doubling method (*Ulaby et al. 1986, Fung 1994*). The study covers effects of snow parameters such as snow layer thickness, volume fraction of scatterers, snow wetness and rms height of snow top boundary. The overall effect of an increase in snow layer thickness results in more volume scattering. The backscattering coefficient is seen to increase over the range of volume fraction of scatterers from 20 % to 40 %. Due to the small spacing between the ice particles and fractional volume of snow is usually between 10 % and 20 % when fresh and may reach 40 % or more after aging. The presence of liquid water in a snow medium increases the absorption of the medium and causes the albedo to decrease. The scattering is weaker when the

snow is wet. The influence of air-snow interface is generally quite small due to the small dielectric discontinuity at air-snow interface except possibly at small angles of incidence. The effect of the boundary between snow and ground is generally larger than the air-snow boundary unless the snow layer is so lossy that this boundary is not seen by the incident wave. In the case of wet snow, the influence of air-snow interface can be significant.

A polarimetric model that includes surface and volume scattering as well as the interaction terms between surface and volume has been developed (*Shi and Dozier 1993, Shi and Dozier 1995*). Radiative transfer model for dense media is used for the volume scattering component. The surface scattering model, IEM, is used to evaluate the surface scattering components and introduced to the radiative transfer equations as the boundary conditions in order to evaluate the importance of the interactions between the surface and volume scattering signals. The results indicate that the surface and volume interaction terms are the important scattering sources for cross polarized signals (*Shi and Dozier 1993, Shi and Dozier 1995*). The surface-volume interaction terms under the independent assumption results in an over-estimation for HH polarization. For VV polarization, however, it always over-estimates at small incidence angles and under-estimates at large incidence angles.

The strong fluctuation theory has been applied to calculate scattering from snow (*Tsang et al. 1982, Jin and Kong 1984*). *Tsang et al. (2003)* applied quasicrystalline approximation (QCA) dense medium theory to calculate the absorption, scattering and emission of snow at multiple frequencies.

### 2.3 Microwave Emission Models for Snow-Covered Terrain

Microwave emission models of snow are based on the solution of the radiative transfer equation. Radiative transfer equation has been extensively applied to studies of multiple scattering and transmission of specific intensity in random media. In the radiative transfer theory, random media may be treated as random

*discrete scatterer media* or *continuous random media*. According to this division, the emission models can be separated into two different approaches:

*The discrete nature of the scattering particles* is simulated by discrete scatterers embedded in a homogeneous layered medium. The discrete scatterers may be treated as spherical *Rayleigh* or *Mie* particles, non-spherical particles (spheroid, disk, cylinder, etc.), or others (*Kong et al. 1979, Tsang and Kong, 1985*). In the model, the radiative transfer theory is used to evaluate the scattering of waves by discrete scatterers. The phase matrix is constructed by assuming that the particles scatter independently. This approach is known as the conventional radiative transfer (CRT) theory. When there is more than one scatterer within the distance of a wavelength, the assumption of independent scattering in the CRT theory is not valid. The dense medium radiative transfer (DMRT) equations have been derived from the wave theory for electromagnetic wave propagation and scattering in dense media. The DMRT emission and scattering model is based on two methods. The first method is the analytic quasicrystalline approximation (QCA) (*Tsang and Kong, 2001*). The second method is Monte Carlo simulations of the exact solution of Maxwell equations (*Tsang et al. 2001*).

The dense medium radiative transfer (DMRT) equations have found their applications in snow modelling (*Tsang 1987, Tsang et al. 1992*). In DMRT, the extinction rate, albedo, and phase matrix are related to the physical parameters of the medium, such as the size, sizes distributions, fractional volume, shape, orientation, and the dielectric properties of the particles. Discrete scattering models are complex. They need more input parameters than the continuous random medium approach. The practical use of the models is limited by the high computing time.

*Continuous random media* are characterized by the variance and correlation function of random fluctuation for the effective permittivity. The effective permittivity is used to characterize randomness and scattering effects in a random medium.

The phase matrix and scattering coefficient of scalar and vector radiative transfer equations can be derived by using either the weak fluctuation theory (*Tsang and Kong 1975, 1976, 1980a, 1985*) or the strong fluctuation theory (*Tsang and Kong 1981a, 1981b, 1982, Stogryn 1986, Jin et al. 1984, Jin 1989, Yueh et al. 1990, Nghiem et al. 1993, 1995, 1996*).

The strong fluctuation theory can be applied to calculate scattering (*Tsang and Kong 1981a, 1981b, 1982, Jin et al. 1984, Yueh et al. 1990, Nghiem et al. 1993, 1995*) or emission (*Stogryn 1986, Jin 1989, Wigneron et al. 1993, Calvet et al. 1994*) from the random media.

A microwave emission model for random medium with non-spherical scatterers was improved by using the radiative transfer equations and the strong fluctuation theory. The model was then applied to describe microwave emission from wet snow (*Huining 2001*).

*The composite discrete-continuous approach* is based on the combination of both discrete approach to simulate single scattering albedo and the continuous approach to simulate the scattering coefficients and the phase matrix (*Wigneron et al. 1995*).

*The TKK snow emission model* (*Pulliainen et al. 1999*) is a semi-empirical approach. The basic assumption in the TKK snow emission model is that the scattering is mostly concentrated in the forward direction. Another example of semi-empirical approach is *microwave emission model of layered snowpacks (MEMLS)* (*Wiesmann et al. 1999*). It is based on the radiative transfer equations, in which the scattering coefficient was determined empirically from measured snow samples, whereas the absorption coefficient, the effective permittivity, refraction and reflection at layer interfaces were based on physical models.

# III Physical and Microwave Characteristics of Snow, Forest and Soil

## 3.1 Physical Properties of Snow, Forest and Soil

Snow is a fine-grained media close to its melting temperature. *Physical properties of snow* consist of snow depth, snow density, liquid water content, stratigraphy, surface features, grain size and grain shape. These physical properties are directly consequences of some important processes, which occur during the metamorphism of a snow. The surface of snow is generally smooth with respect to microwaves. It becomes rougher a as result of changing meteorological conditions such as wind action and melt erosion. Snow shows a stratified profile such as layers of different types of grains, density, and wetness. The grains are generated by precipitation (snowflakes, snow crystals) possibly under the influence of wind or deposition. The grains embedded in snow change in size and shape by different kinds of metamorphism *(Rott et al. 1988)*. Equi-temperature metamorphism is distinguished by the transport of water vapor from regions of high surface energy to regions of lower surface energy in a snow with constant temperature below freezing. Uniform, well-rounded larger grains in size are produced. Equi-temperature metamorphism is connected with a large timescale such as months. During temperature-gradient metamorphism water vapor under a strong temperature gradient is transported from the warmer (lower) to the colder (upper) layers by sublimation and deposition. The result is well-oriented grains whose form reflects the temperature and vapor pressure gradients. In melt-freeze metamorphism when the snow at freezing point begins to melt the melt water is trapped between the grains. Refreezing results in a denser snow. Repeated melt-freeze cycles lead to very large grains. Snow can be divided into three categories: dry snow, wet snow and refrozen snow. Dry snow is a mixture of air and ice particles. Wet snow is a mixture of air, ice and water. Refrozen snow is a mixture of air and large snow grains, which were formed by melt-freeze metamorphism.

Typical physical properties of snow are as follows:

- Snow density = 0.1-0.4 g / $cm^3$
- Liquid water content = 0-10% (dry snow to wet snow)
- Ice grain radius for dry snow = 0.1-0.5 mm
- Water inclusions radius = 0.1-2 mm

Examples of grain size, shapes and layer structure of snow can be found in *Vallese and Kong (1981)*, *Roth et al. (1988)*, *Kurvonen (1994)*, and *Weise (1996)*. Examples of the shape of liquid water inclusions can be found in *Sihvola (1999)*.

Microwave backscatter from forest is very sensitive to the orientation and size distribution of leaves, branches, trunks and moisture content of forest canopies. These physical parameters represent discrete scattering and absorbing elements in forest canopy. Dielectric constant of vegetated surfaces include temperature of the scattering medium, relative moisture content of vegetation, soil, and snow cover, and the presence of water on vegetation determine the magnitude and phase of the electromagnetic wave scattered from forest and received by microwave sensors. The importance of forest canopy elements regarding microwave scattering and absorption elements depends on frequencies. At P- and L-bands, microwave scattering and absorption are due to tree trunks and larger branches within forests, as well as the ground surface. At these wavelengths, the smaller stems and the foliage act mainly as attenuators. At C- and X-bands, microwave scattering and absorption are due to smaller branches and leaves and needles in the forest canopy. Polarization combination of the received signal is very much related to polarization of the transmitted signal and horizontal / vertical orientation of scattering elements in forest canopy.

Boreal forests in Finland differ from those in central Europe in three important aspects: 1) the stem volume (density of forest) is lower, 2) dominant species are conifers (Scots pine and Norwegian spruce), and 3) the most usual soil type is moraine (*Pulliainen et al. 1994*). The average stem volume per hectare in forested

land is about 100 $m^3$/ha in southern Finland and only about 50 $m^3$/ha in northern Finland, whereas the average stem volume may exceed 200 $m^3$/ha in central European forest regions. Both the low average stem volume and the predominant moraine soil type increase the applicability of C-band radar for forest applications in Finland (*Pulliainen et al. 1996*).

*A soil medium* is a mixture of soil particles, air voids and liquid water. Soil moisture is one of the most important physical parameters in microwave remote sensing of soil. In most natural settings, the effect of roughness may be equal to or greater than the effect of soil moisture on radar backscatter. A soil under dry snow cover is typically frozen. A frozen soil medium is a mixture of soil particles, free water, bound water, and ice particles. Bound water refers to the water molecules, which may be strongly bound to soil particles not allowing the usual rotational states of $H_2O$ molecules in liquid water (*Hallikainen et al. 1985, Dobson et al. 1985*).

The most usual soil type in Finland is moraine. In moraine soil, the moisture level of the top layer is considerably lower than in clay soil.

### 3.2 Microwave Properties of Forest and Soil

Microwave backscatter models treat a forest stand either as a set of continuous horizontal layers (*Richards et al. 1987, Durden et al., 1989, Ulaby et al., 1990, Chauhan et al. 1991*) or as a discontinuous layer with individual trees acting as distinct scattering centers (*Sun et al., 1991, McDonald and Ulaby, 1993*). Both models calculate the same major scattering terms: (1) volume scattering from the tree canopy (the branches and leaves/needles); (2) direct ground scattering; (3) ground-to-trunk scattering; (4) ground-to-crown scattering; and (5) ground-to-crown-to-ground scattering. Most models assume that the tree trunks and branches can be modeled as lossy dielectric cylinders, and the leaves or needles as dielectric discs or cylinders, respectively.

The permittivity of vegetation is given as a function of the volumetric moisture content $M_v$ with the following equation (*Fung 1994*):

$$\varepsilon(M_v) = \varepsilon_n + vf_f\{4.9 + 75/[1 + j(f/18)] - j(18\sigma/f)\} + vf_b\{2.9 + 55/[1 + (jf/0.18)^{0.5}]\} \quad (3.2.1)$$

where $f$ is frequency, $\sigma$ is the conductivity $\varepsilon_n$ is the nondispersive residual component of the dielectric constant, $vf_f$ is the free-water volume fraction, $vf_b$ is the volume fraction for bound water and given following equations:

$$\varepsilon_n = 1.7 + 3.2M_v + 6.5M_v^2 \quad (3.2.2)$$

$$vf_f = M_v(0.82M_v + 0.166) \quad (3.2.3)$$

$$vf_b = (31.4M_v^2)/(1 + 59.5M_v^2) \quad (3.2.4)$$

*Pulliainen et al. (1994)* has studied the backscattering properties of boreal forest using empirical airborne and spaceborne radar data from Finland. The obtained results show that the radar response to the forest stem volume (biomass) is relatively low at both C- and X-bands. The change was on order of 2-2.5 dB as the stem volume changed from 0 to 370 $m^3$/ha.

*Macelloni et al. (2001)* has studied multifrequency (from L- to Ka-band) microwave emission from forest stand in Italy. The use of the highest frequencies (Ka and X) has been successful in distinguishing different forest types, whereas L-band has been found to be the best frequency for estimating woody volume and basal area.

*Microwave properties of a soil surface* are dominated by its geometry and its permittivity or dielectric constant. The permittivity itself depends strongly on the soil moisture content because of the very high permittivity of liquid water. The permittivity properties of soil have been studied by many authors (*Hallikainen et*

*al. 1985, Dobson et al. 1985, Peplinski et al. 1995, Mätzler 1992, Tikhonov 1994*). Both active and passive microwave remote sensing can accurately measure surface soil moisture contents in the top few cm of the soil. At L-band (1 to 2 GHz), the dielectric constant can vary from about 3 for dry soil to about 20 for wet soil, which can result in a decrease in emissivity for passive systems from about 0.95 to 0.6 or lower and an increase in the radar backscatter approaching 10 dB (*Ustin 2004*). Surface emissivities typically are also sensitive to surface roughness. For active microwave remote sensing of soils, the measured radar backscatter is related directly to soil moisture but is also sensitive to surface roughness. The sensitivity of active microwave sensors to soil moisture was demonstrated with ground-based, airborne, and even some spaceborne experiments (*Ulaby and Batlivala 1976, Ulaby et al. 1978, Chang et al. 1980, Jackson et al. 1981, Wang et al. 1986, Dobson and Ulaby 1986, Lin et al. 1994a, 1994b*). The approach adopted by *Oh et al. (1992)* is based on scattering behavior in limiting cases and on experimental data. They have developed an empirical model in terms of the root mean square (rms) roughness height, the wave number, and the relative dielectric constant. By using this model with multipolarized radar data, the soil moisture content and the surface roughness can be determined. An algorithm was derived that uses L-band HH and VV radar cross sections only to estimate surface roughness and soil moisture (*Dubois et al. 1995*). In this case, the algorithm was tested with both airborne and spaceborne SAR data and an absolute accuracy of 3-4 % was found for surfaces with vegetation that has a normalized difference vegetation index (NDVI) < 0.4.

*Nolan and Fatland (2003)* investigated the relationship between soil moisture and the penetration depth of SAR at L-, C-, and X-bands. They found this relationship to be nonlinear and that a change of 5 % volumetric water content can cause 1 to 50 mm of change in C-band penetration depth depending on initial volumetric water content of soil.

### 3.3 Microwave Properties of Snow

Microwave properties of snow are closely related to understanding the relations between the electromagnetic interactions in different parts of the spectrum and the physical snow properties. The relationship between backscattering and physical snow properties is controlled by the scattering mechanism. At C-band, backscattering is controlled by snow volume backscattering and the surface backscattering at air - snow interface. When wetness is low, the dielectric contrast between air and snow is small and volume scattering dominates, so backscattering is not sensitive to surface roughness. As snow wetness further increases, backscattering becomes sensitive to surface roughness. This is because the surface scattering component becomes dominating, resulted from rapidly increasing surface scattering component and decreasing volume scattering component. At long wavelength (L-band with 24 cm wavelength) snow particle size has little effect on the backscattering signals from a dry snow cover. The scattering mechanism can be considered as a homogeneous dielectric layer (snow) over a rough surface. The relationships between backscattering signals and snow water equivalent can be either positive or negative depending on the snow physical parameters, ground surface parameters and incidence angle. In addition to snow density and ice particle size, size variation, snow stratification, and underlying ground conditions affect the interpretation of the observed backscattering signals.

### 3.3.1 Correlation Functions and Lengths of Snow

The correlation function and correlation lengths are associated with the physical structure of the media. In the correlation function of snow, the variances characterize the strength of the permittivity fluctuation in snow and the correlation lengths correspond to the scale of the fluctuation. A common parameter for describing the inclusions such as ice particles and water particles in snow is the effective size of particles. To determine the effective size of particles is not an easy problem due to the highly different shapes. The correlation lengths can be only measured by using image analysis for snow samples.

Generally, a spatial autocorrelation function ACF($\vec{r}$) in three dimensions is defined by (*Mätzler 1997*):

$$\mathrm{ACF}(\vec{r}) = \frac{1}{V}\iiint_{V} f(\vec{r}') \cdot f(\vec{r}'-\vec{r})\, d^3\vec{r}' \tag{3.3.1}$$

where f($\vec{r}$) is a spatially fluctuating function of position $\vec{r}$, $\vec{r}'$ is the displacement, V is the total volume of the medium under investigation; f($\vec{r}$) is normalised so that ACF(0)=1. In the surface model such as Integral Equation Model (IEM), f($\vec{r}$) is the surface profile z(x) (in one-dimensional case). Autocorrelation function ACF(x) is a measure of the similarity between the height z at a point x and a point x' away from x. Dealing with the interaction between the electromagnetic radiation and a random media such as in strong fluctuation theory, f($\vec{r}$) represents the medium's permittivity $\varepsilon(\vec{r})$ for a given location $\vec{r}$ in space.

Many autocorrelation functions are assumed to be of exponential form (*Debye 1957, Valleese and Kong 1981*). It can be written as form (*Weise 1996*):

$$\mathrm{ACF}(r) = \exp(-\frac{r}{l}) \tag{3.3.2}$$

where l is called the correlation length.

ACFs were calculated for spheres, spherical shells and ellipsoids (oblate spheroids or disk like shapes and prolate spheroids or needle like shapes) in (*Mätzler 1997*). For spheres, the correlation function is (*Mätzler 1997*):

$$\mathrm{ACF(r)} = \begin{cases} 1 - 3\mathrm{r}/4\mathrm{a} + (\mathrm{r}/\mathrm{a})^3/16 & \mathrm{r} < 2\mathrm{a} \\ 0 & \mathrm{r} \geq 2\mathrm{a} \end{cases} \tag{3.3.3}$$

where a is the grain radius.

For the case of penetrable sphere, the normalised correlation function is (*Lim et al. 1994*):

$$\mathrm{ACF(r)} = \begin{cases} \frac{1}{\mathrm{f}}(1-\mathrm{f})^{\left[3\mathrm{r}/4\mathrm{a}-(\mathrm{r}/\mathrm{a})^3/16\right]} - \frac{1}{\mathrm{f}}(1-\mathrm{f}) & \mathrm{r} < 2\mathrm{a} \\ 0 & \mathrm{r} \geq 2\mathrm{a} \end{cases} \tag{3.3.4}$$

where a is the radius and f the volume fraction of the spheres. If $\mathrm{f} \to 0$, *Lim's* model and *Mätzler's* model are identical. Gaussian correlation function can be written as (*Tsang and Kong 1981*):

$$\mathrm{ACF(r)} = \exp\left(-\frac{\mathrm{r}^2}{\mathrm{L}^2}\right) \tag{3.3.5}$$

Some applications of strong fluctuation theory suggest that the ACF is exponential form in vertical direction and Gaussian form in horizontal (*Jin 1989, Tsang and Kong 1981, Calvet et al. 1994, Wigneron et al. 1993, Ulaby et al. 1986*).

$$\mathrm{ACF(r)} = \exp\left(-\frac{\mathrm{x}^2+\mathrm{y}^2}{\mathrm{L}_\mathrm{p}^2} - \frac{|z|}{\mathrm{L}_z}\right) \tag{3.3.6}$$

Anisotropic correlation function with azimuthal symmetry is given (*Yueh and Kong 1990* ):

$$\mathrm{ACF(r)} = \exp\left(-\sqrt{\frac{\mathrm{x}^2+\mathrm{y}^2}{\mathrm{l}_\mathrm{p}^2} + \frac{\mathrm{z}^2}{\mathrm{l}_\mathrm{z}^2}}\right) \tag{3.3.7}$$

where $l_p$ is the correlation length in horizontal direction and $l_z$ is the correlation length in vertical direction. A general case for Equation (3.3.5) for random media with ellipsoidal scatterers is (*Nghiem et al. 1993, Nghiem et al. 1995, Nghiem et al. 1996*):

$$ACF(r) = \exp\left(-\sqrt{\frac{x^2}{l_x^2} + \frac{y^2}{l_y^2} + \frac{z^2}{l_z^2}}\right) \quad (3.3.8)$$

where $l_x$, $l_y$, $l_z$ are the minor, the meridian and the major axes of the scatterer in the local co-ordinates respectively.

### 3.3.2 Effective Permittivity of Snow

An effective permittivity describes propagation and attenuation in the media. The relative effective permittivity of most natural materials, when dry, is between 3 and 8 (for a typical radar frequency). For such values, the penetration depth is quite large and the reflectivity correspondingly small. The permittivity for water, on the other hand, is around 80 resulting in high reflectivity from the surface and almost no penetration. The effective permittivity for a material varies almost linearly with the moisture content per unit volume. The higher the moisture content, the smaller the penetration depth is and the greater the reflectivity is. Since the effective permittivity depends on the frequency of the electromagnetic wave, so does the reflectivity. The higher the frequency (or the smaller the wavelength), the smaller the penetration is.

The effective permittivity of snow is a function of frequency, temperature, volumetric water content, snow density, ice-particle shape and the shape of the water inclusions. Snow can be modeled as a mixture of constituents, which exhibit a variety of dielectric characteristics. Dry snow is a mixture of air and ice and wet snow is a mixture of air, ice and water.

In theoretical backscattering modeling of the terrain, calculation of the effective permittivity of a random medium is essential. Investigation of the effective permittivity of snow has a long history. Experimental studies of the effective permittivity of snow started in 1952 (*Cumming 1952*) and were followed by many others (*Glen and Paren 1975, Colbeck 1980, Ambach and Denoth 1980, Tiuri et al. 1984, Mätzler et al. 1984*). A summary of the semi-empirical dielectric models

of snow is found in (*Hallikainen et al. 1986*). Sihvola (1999) derived general mixing formulas of the effective permittivity for discrete scatterers immersed in a host medium.

The simple mixing models that relate the effective permittivity of the mixture to the permittivities of the constituent (inclusions and host) describe the situation well enough if the size of the inclusions is much smaller than the wavelength and if their shape is known. The empirical models are also confined by the frequency.

In order to investigate the dielectric properties of snow at higher frequencies the strong permittivity fluctuation theory for snow cover was introduced in 1986 (*Stogryn 1986*) and its application to calculate the effective permittivity has been reported by many authors (*Tsang 1982, Yueh and Kong 1990, Lim et al. 1994, Nghiem et al. 1993, Nghiem et al. 1995*).

Using the strong fluctuation theory, an inhomogeneous layer can be modeled as a continuous medium. Snow is described by a correlation function, with the variance characterizing the strength of the permittivity function of the medium. The correlation function contains information on the physical parameters of discrete particles, such as size, shape; it is approximately represented by correlation lengths corresponding to the scales of the fluctuation in horizontal and vertical directions (*Lim et al. 1994, Vallese and Kong 1981, Mätzler 1997*).
Once the grain size and shape, fraction volume (or snow density), permittivity of the layer background, permittivity of the scatterer (ice particles) embedded in the layer and frequency are given using the strong fluctuation theory, we can calculate the effective permittivity of snow. Note that the imaginary part of the permittivity of the scatterer (ice particles) depends on temperature and frequency; hence, the effective permittivity of snow based on strong fluctuation theory also depends on temperature and frequency.
Consider scatterers with permittivity $\varepsilon_s$ embedded in a background medium with permittivity $\varepsilon_b$. For the case of dry snow, the scatterers are ice particles and the

background is air. The fraction volume occupied by the scatterers is $f_v$ and the fraction volume occupied by the background medium is $1-f_v$. From the point of view of random medium theory, the medium is characterized by a random permittivity (*Tsang and Kong 1981a, 1981b*):

$$\varepsilon(\bar{r})=\varepsilon_m+\varepsilon_f(\bar{r}) \tag{3.3.9}$$

$$\langle\varepsilon(\bar{r})\rangle=\varepsilon_m \tag{3.3.10}$$

$$\langle\varepsilon_f(\bar{r})\rangle=0, \tag{3.3.11}$$

where $\bar{r}$ is the position vector, $\varepsilon_m$ the average permittivity and $\varepsilon_f(\bar{r})$ the spatially fluctuating permittivity. The angular bracket < > stands for ensemble average and corresponds to spatial average on account of the ergodic theorem. Thus, $P_r(\varepsilon(\bar{r})=\varepsilon_s)=f_v$ and $P_r(\varepsilon(\bar{r})=\varepsilon_b)=1-f_v$, where $P_r$ stands for probability. The random process is non-Gaussian, as $\varepsilon(\bar{r})$ can have either of the two values $\varepsilon_s$ and $\varepsilon_b$.

The correlation function of the fluctuation of $\varepsilon_f(\bar{r})$ is (*Tsang and Kong 1981a, 1981b*):

$$\langle\varepsilon_f(\bar{r})\varepsilon_f(\bar{r}')\rangle=\delta\varepsilon_m^2\, ACF(\bar{r}-\bar{r}') \tag{3.3.12}$$

where δ is the normalized variance of the fluctuations and $ACF(\bar{r}-\bar{r}')$ is the normalized correlation function with $ACF(0)=1$.

In terms of the medium properties (*Tsang and Kong 1981a, 1981b*):

$$\varepsilon_m=(1-f_v)\,\varepsilon_b+f_v\,\varepsilon_s \tag{3.3.13}$$

$$\delta=\frac{(\varepsilon_b-\varepsilon_m)^2(1-f_v)+(\varepsilon_b-\varepsilon_s)^2 f_v}{\varepsilon_m^2} \tag{3.3.14}$$

We should note that the effective permittivity $\varepsilon_{eff}$ is not equal to the average permittivity $\varepsilon_m$.

# IV Results and Discussion

## 4.1 Microwave Radar Backscattering Signatures of Snow

In [**P1**], the backscattering coefficients for snow-covered and snow-free non-forested (open) areas were calculated as average values for sample plots of 25 m by 25 m along the test site center lines, where the snow ground truth measurements were conducted, using an interval of 100 meters. The empirical SAR data were acquired by EMISAR of Technical University of Denmark near the city of Oulu in Northern Finland during the European Multisensor Airborne Campaign 1995 (EMAC'95). Airborne measurements were conducted on 22 and 23 March, on 2 and 3 May 1995. The correlations between snowpack parameters and the backscattering coefficients are computed at C-and L-band for all polarizations. A statistical analysis is carried out between the backscattering coefficient and snow water equivalent for the chosen sample plots. The analysis covers two situations (March and May), three snow test sites (1, 2 and 4) and all polarizations for both C-and L-band. Test site 3 is forested area and did not have non-forested areas (open). Hence it was not considered in the analysis. The results show that the correlation coefficients are higher at C-band than L-band, obviously due to stronger interaction of the radar signal with the snow cover. The level of backscatter is higher at C-band than L-band for high snow water equivalent values at all polarizations. On the other hand, there is no clear separation between C-and L-band for low snow water equivalent values. This may be due to the high contribution of the snow-ground interface.

In [**P1**], the development of an empirical model is presented to retrieve the snow water equivalent from C-band SAR data in non-forested (open) areas. Total backscattering coefficient $\sigma^0$ of dry snow is modeled empirically by fitting the data with a linear expression:

$$\sigma^0 = a.swe + b\,, \tag{4.1}$$

where *a* and *b* are constant coefficients and *swe* is snow water equivalent of dry snow (mm). The coefficients were determined by the least square sum fitting of (4.1) to the measurement data as follows,

$$\sum_{i=1}^{N}\left(\sigma^0_{i,MEAS}-\sigma^0_{i,MODEL}(swe,a,b)\right)^2 = \ minimum \tag{4.2}$$

where $N$ is the number of training sample plots of dry snow, $\sigma^0_{i,MEAS}$ is the measured mean backscatter for sample plot *i* of dry snow and $\sigma^0_{i,MODEL}(swe,a,b)$ is the modeled backscatter for sample plot *i* of dry snow.

This is a simple data fitting experiment in order to see if there is any correlation between the backscattering coefficient $\sigma^0$ of dry snow and snow water equivalent parameter. A comparison between 108 averaged data for *swe* in 20 mm intervals such as 0 - 20, 21 – 40, etc. and model at C-band for three polarizations is shown in Figure 4.1. Scatter of the data points at CVV- band is much smaller than at CVH band. This may cause the high correlation at CVV band. CHH has also the data points almost as sparse as CVH which may explain smaller correlation. The data points were selected from agricultural land (non-forested). Any existing vegetation may cause some errors. The vegetation could increase the scatter and decrease correlation. This effect is higher at cross-polarization than at co-polarization.

Since the empirical model presented in this study is able to estimate values for snow-covered terrain in a reasonable manner, we can invert the model to obtain snow water equivalent as follows,

$$swe = \frac{\sigma^0_{MEAS}-b}{a}, \qquad \text{IF} \quad \sigma^0_{MEAS} > b$$
$$\text{ELSE} \qquad swe = 0 \tag{4.3}$$

Results from the retrieval of snow water equivalent at C-band VV polarization are shown in Figure 4.2. The data used for the retrieval of snow water equivalent is

the testing data that is 50% of the all data set. The RMSE values are 71 mm, 77mm and 88 mm for VV, VH and HH polarization, respectively. The best fit with the data is obtained using VV polarization. Although the possibility to determine SWE with an RMSE of 71 mm seems to be of little practical use this is good information in various polarizations and the results would be much better without a couple of data points.

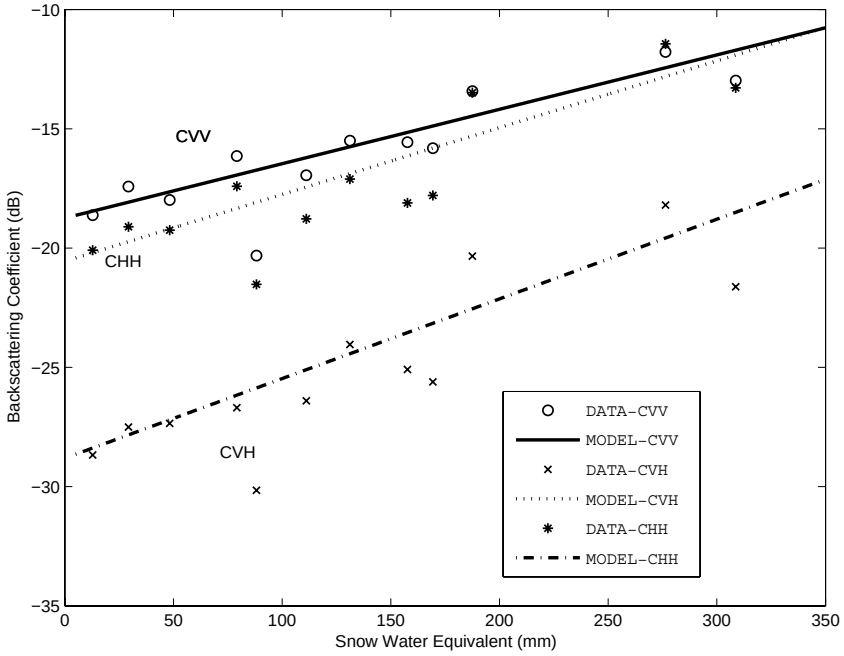


Figure 4.1 Comparison between the averaged data for SWE in 20 mm intervals and model at C-band for three polarizations. The model lines show the empirically modeled (see Eq. 4.1) responses by using training data.

It was shown that dry snow can be discriminated from bare ground by using ERS-1 C-band SAR data (*Bernier and Fortin, 1992*) and , on the contrary, it was also reported that dry snow could not be discriminated from bare ground when single polarization data is used (Koskinen et.al, 1997). The limitations for application of C-band backscatter intensities to retrieve snow water equivalent because of the weak signal of dry snowpack was also reported in EnviSnow final report (*Malnes, E., 2005*). The estimation of snow water equivalent by using dual-frequency polarimetric SAR data has been studied with promising results (*Shi and Dozier, 1996*).

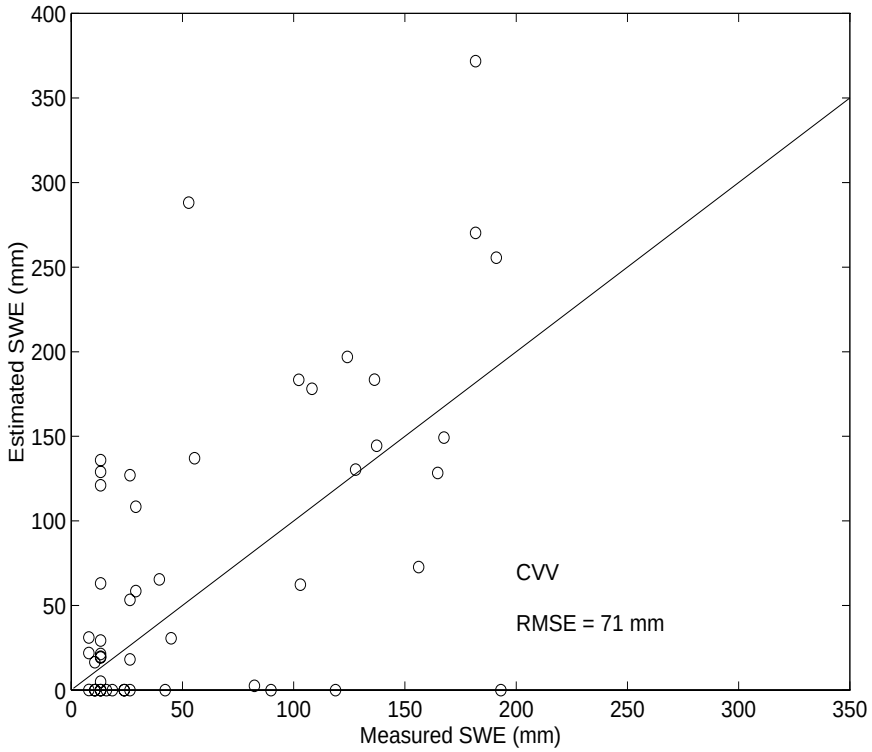


Figure 4.2 Comparison of estimated (Eq. 4.1) and measured snow water equivalent values using the C-band, VV polarization algorithm.

Figure 4.3 shows that our model gives better results when the data were averaged over the test site. In the EnviSnow final report (*Malnes, E., 2005*) C-band data were not averaged at all and, thus, no retrieval of SWE seemed possible. The number of averaged data points is 88, 17, and 3 for test site 1, 2, and 4 respectively. The difference between estimated and measured snow water equivalent values is in range of 14 %, 6 %, 5 % for test site 1, 2 and 4 respectively.

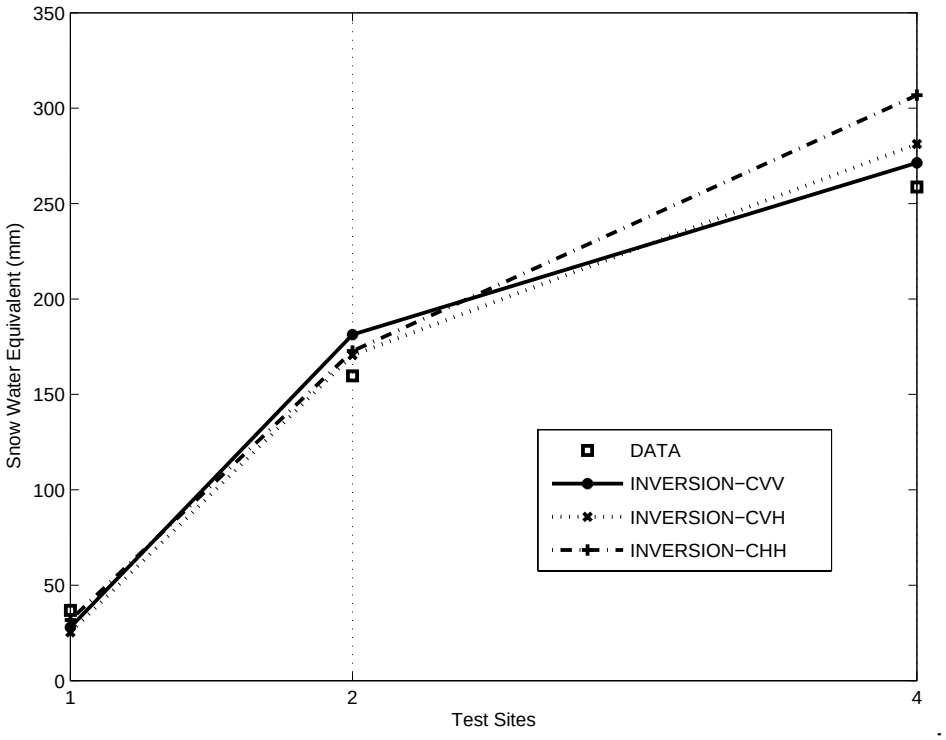


Figure 4.3 Comparison of estimated and measured averaged snow water equivalent for test sites, 1, 2 and 4, respectively.

### 4.2 Semi-Empirical Backscattering Model for a Forest-Snow-Ground System

The main problem with the forest canopy models is the complexity of the target. The more accurately the model includes the physical features of the target, the larger is the number of parameters needed. Empirical models typically have a substantially smaller number of parameters than theoretical models. Semi-empirical models can basically combine benefits of both modeling approaches. In [**P2**], a C-band semi-empirical backscattering model is presented for the forest-snow-ground system. The backscattering coefficients for snow-covered and snow-free forested areas were calculated as average values for sample plots of 25 m by 25 m along the test site center lines, where the snow ground truth measurements were conducted, using an interval of 100 meters during the European Multisensor Airborne Campaign 1995 (EMAC'95) in northern Finland same as in [**P1**] . The analysis covers two situations (March and May), two forested test sites (2 and 4) and all polarizations for both C-and L-band.

The average backscattering coefficient of forested land-cover can be approximately modeled ignoring trunk-ground and multiple scattering mechanisms (*Pulliainen et. al 1996, Pulliainen et. al 1999*).

In [**P2**], we also used an empirical boreal forest canopy transmittivity model which was developed on the basis of passive microwave measurements (*Kruopis et. al 1999*). Airborne passive-microwave data was collected in Northern Finland during EMAC'95. Profiling passive-microwave data were acquired by the TKK (Helsinki University of Technology) radiometer HUTRAD onboard the TKK Short Skyvan aircraft. On March 22, two measurement flights were conducted along the test lines in opposite directions. During the first flight, the radiometer system operated at 6.8 GHz and 18.7 GHz. While flying back, the 10.65-GHz channel was used, along with the 18.7 GHz. The receivers measured both vertically and horizontally polarized radiation. The incidence angle of the antenna beam was set to 50 degree off nadir. During the data collection, the nominal flight altitude was 300 meter and the nominal flight speed was 110 knots (≈59m/s), which resulted in footprint sizes 41 x 93, 26 x 70, and 30 x 77 at 6.8, 10.65 and 18.7 GHz, respectively.

The total backscattering coefficient is calculated by using the forest canopy semi-empirical backscatter model and the empirical ground model. Figure 4.4 shows the total backscattering coefficients data, the total backscattering model and backscattering contributions from the forest canopy backscatter model and the ground floor as a function of stem volume at 5.3 GHz, VV polarization, $50^{o}$ incidence angle. The difference between Figure 4.4 (a) and (b) is the forest canopy transmissivity. The canopy backscatter model shown in Figure 4.4 (a) includes the forest transmissivity model developed on the basis of passive microwave measurement (*Kruopis et. al 1999*). The backscatter model shown in Figure 4.4 (b) includes the forest canopy transmissivity model developed on the basis of radar data (*Pulliainen et. al 1996, Pulliainen et. al 1999*). The behavior of ground backscattering data versus stem volume in Figure 4.4 is as expected; backscattering decreases when stem volume increases.

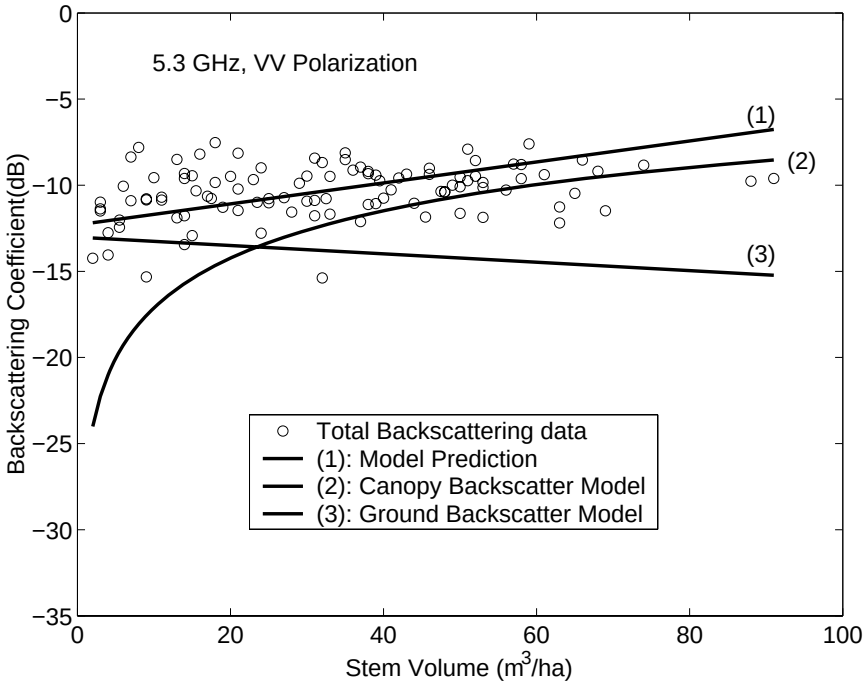


(a)

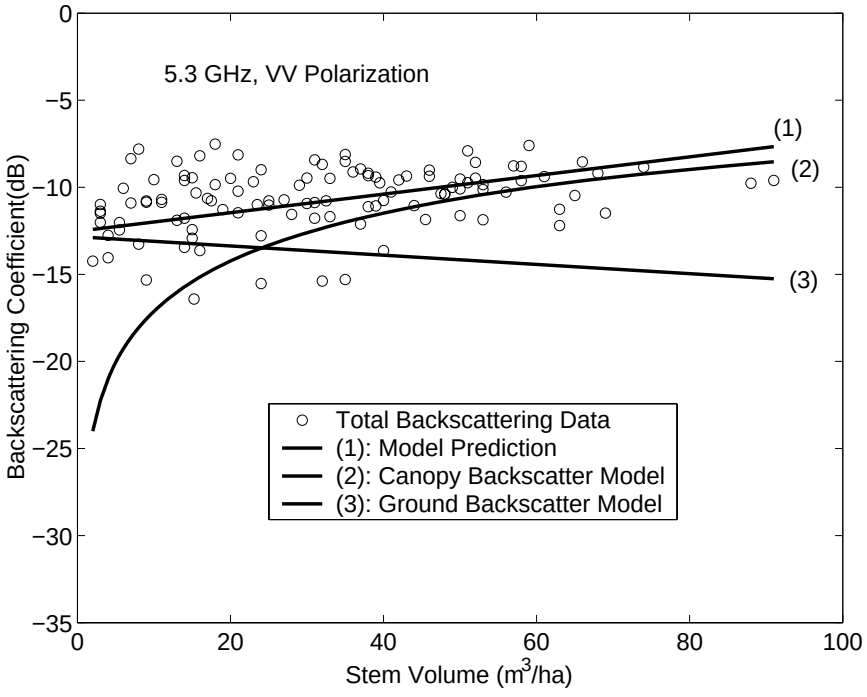


(b)

Figure 4.4 Computed backscattering contributions as a function of stem volume at 5.3 GHz, VV polarization: (a) the forest transmissivity model developed on the basis of passive microwave measurement (*Kruopis et. al 1999*) (b) the forest transmissivity model developed on the basis of radar data (*Pulliainen et. al 1996, Pulliainen et. al 1999*).

In [**P2**], the semi-empirical backscattering model approach for a forest-snow-ground system is shown by combining the semi-empirical and empirical models developed on the different data sets of passive and active sensors. The results of the empirical backscattering modeling of snow and the semi-empirical backscattering modeling of forest canopy covered by snow presented in [**P2**] are important due to the following reasons:(a) backscattering modeling of snow using SAR data is still under study by many researchers and different results have been published in the literature, (b) because of the availability of empirical data (even though it is very limited) on forest-snow-ground system, the developed semi-empirical backscattering model with applicability of the forest transmissivity formulas developed by using the different data sets of passive and active sensors may give a better understanding of forest-snow-ground system for future studies.

### 4.3 Effective Permittivity of Wet Snow

In [**P3**], the strong fluctuation theory is applied to calculate the effective permittivity of wet snow by a two-phase model with non-symmetrical inclusions. Wet snow is treated as a two-phase mixture, where the water is considered as inclusions embedded in dry snow that is the background material. The shape of the water inclusions is taken into account by using an anisotropic azimuthally symmetric correlation function. The effective permittivity is calculated by using a two-phase strong fluctuation theory model with non-symmetrical inclusions. The three-phase strong fluctuation theory model with symmetrical inclusions is presented for theoretical comparison. The results are compared with the Debye-like semi-empirical model and a comparison with the experimental data at 6, 18 and 37 GHz is also presented (*Hallikainen et. al 1986*).

Figures 4.5 to 4.7 show the effect of the size and shape of the water inclusions on the effective permittivity of wet snow at 6, 18 and 37 GHz. The results are shown separately for the real and imaginary part of the effective permittivity of wet snow. The effect of the size and shape of water inclusions on the effective permittivity of wet snow is seen clearly at the three frequencies. When the

correlation length in horizontal direction $l_\rho$ is set to be 0.1mm and the correlation length in vertical direction $l_z$ is changed from 0.2 mm to 1 mm, the effective permittivity of wet snow increases at all 6, 18 and 37 GHz with increasing $l_z$. The increase is significant for high snow wetness values. However, the magnitude of increase, from $l_\rho$ = 0.1 mm and $l_z$ = 0.2 mm to $l_\rho$ = 0.1 mm and $l_z$ = 1 mm, decreases when the frequency increases from 6 GHz to 37 GHz. The effective permittivity of wet snow decreases as $l_\rho$ increases from 0.1 mm to 0.3 mm. The decrease is more significant when the frequency changes from 37 GHz to 6 GHz. These results indicated that the size and shape of the water inclusions are important to take into account for calculating the effective permittivity of wet snow.

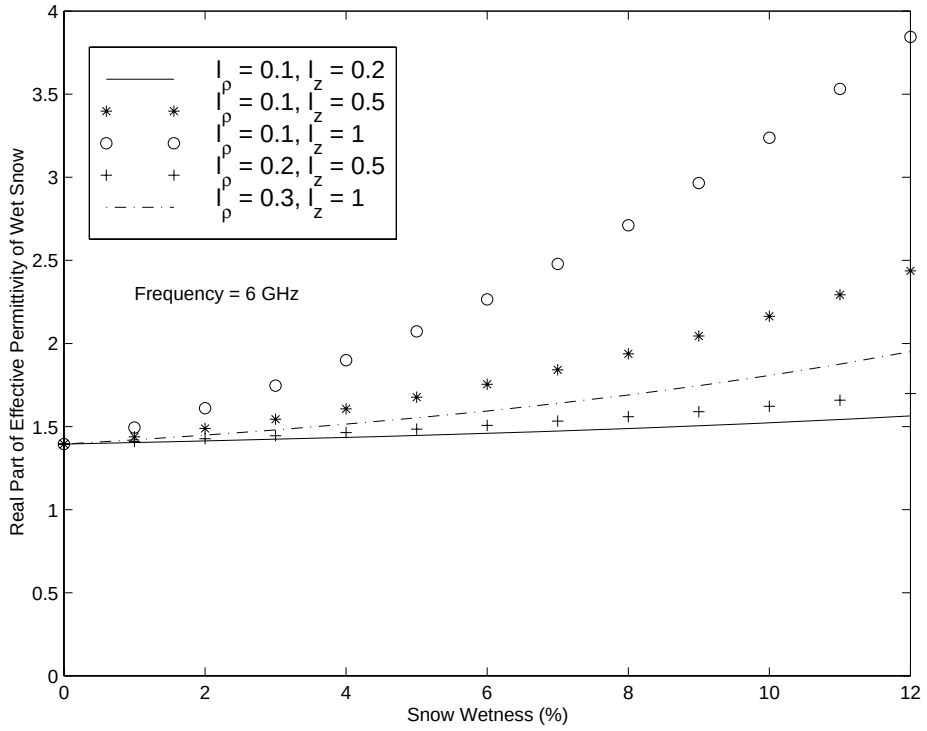


(a)

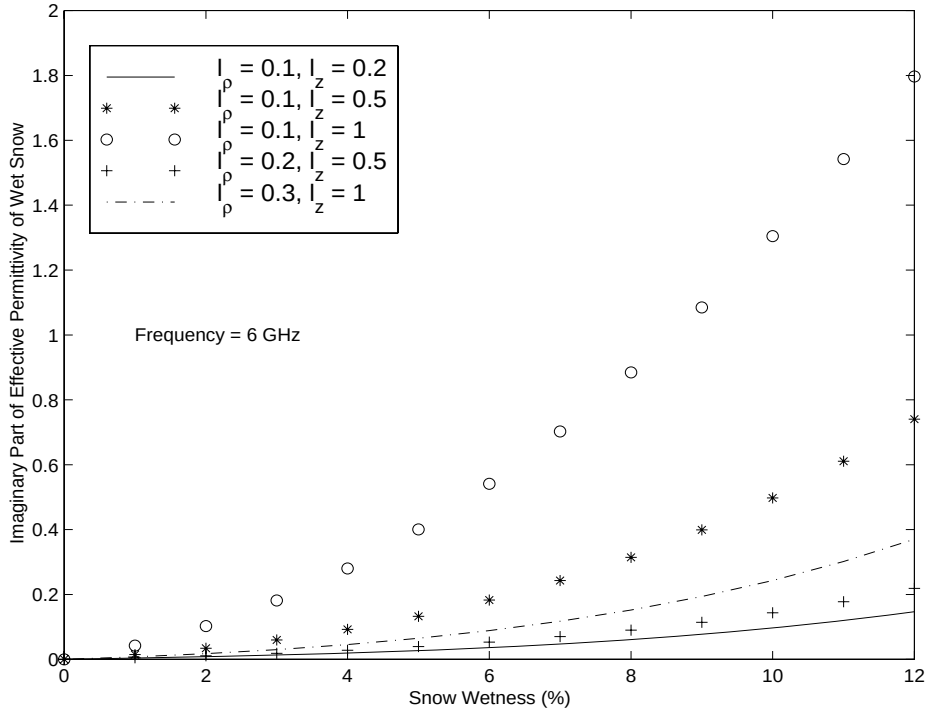


(b)

Figure 4.5 Computed effective permittivity of wet snow at 6 GHz with various correlation lengths (in mm). (a) Real part of the effective permittivity. (b) Imaginary part of the effective permittivity.

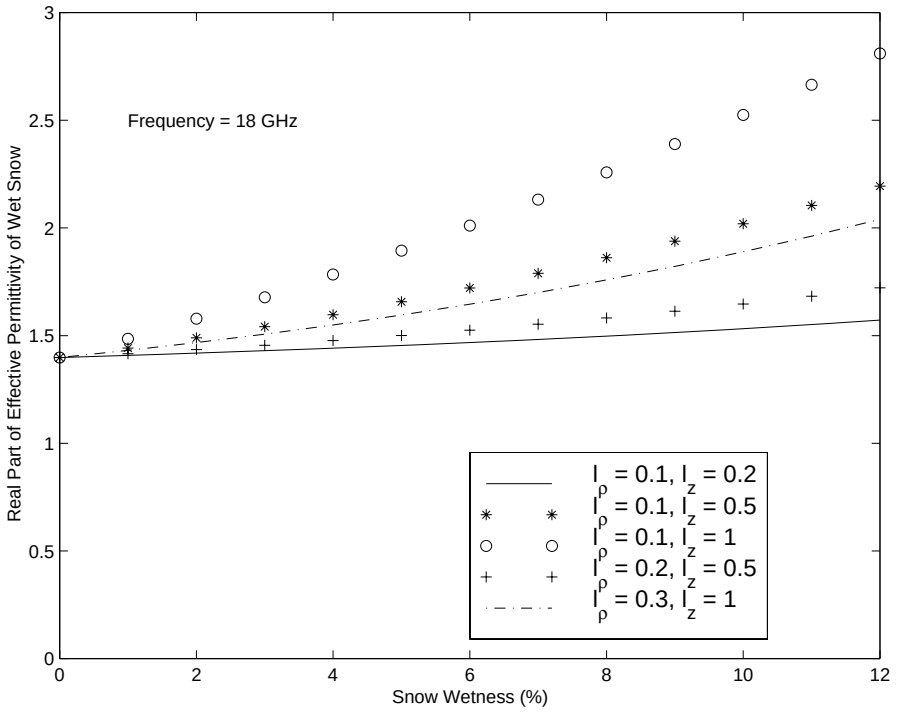


(a)

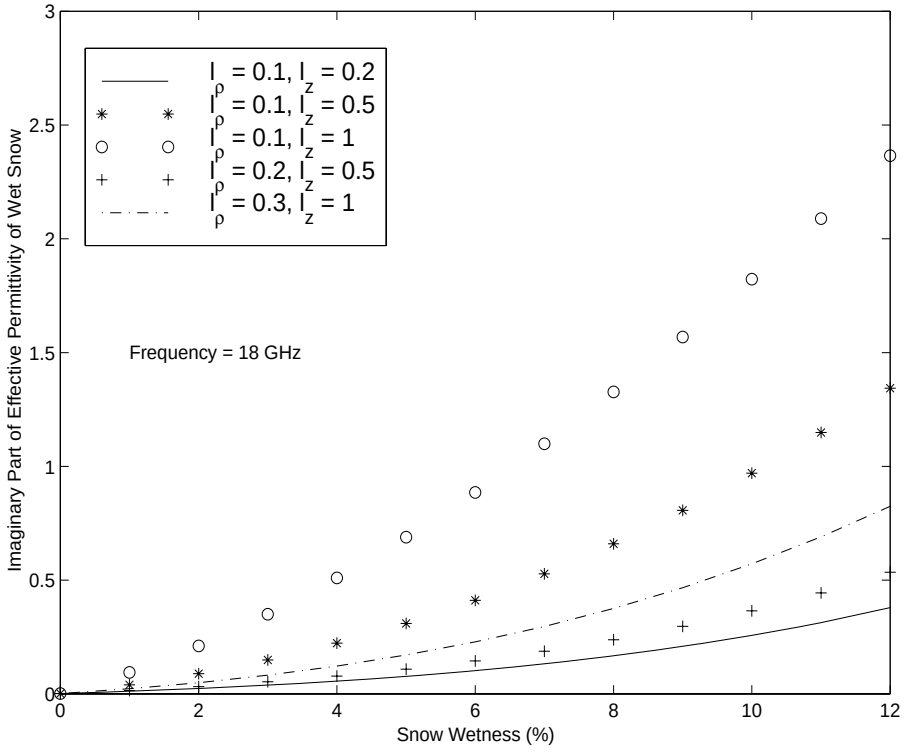


(b)

Figure 4.6 Computed effective permittivity of wet snow at 18 GHz with various correlation lengths (in mm). (a) Real part of the effective permittivity. (b) Imaginary part of the effective permittivity.

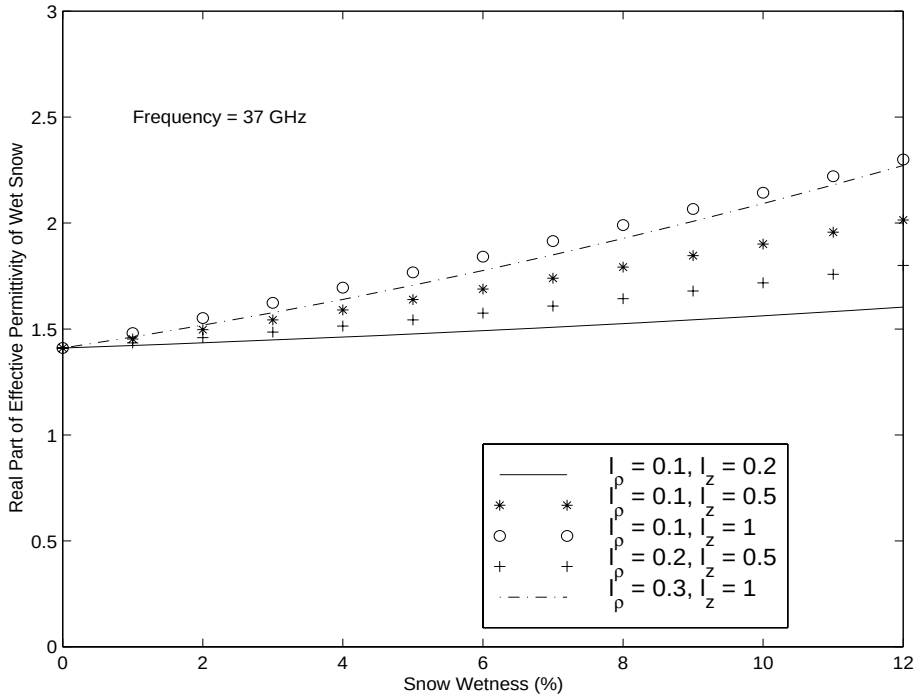


(a)

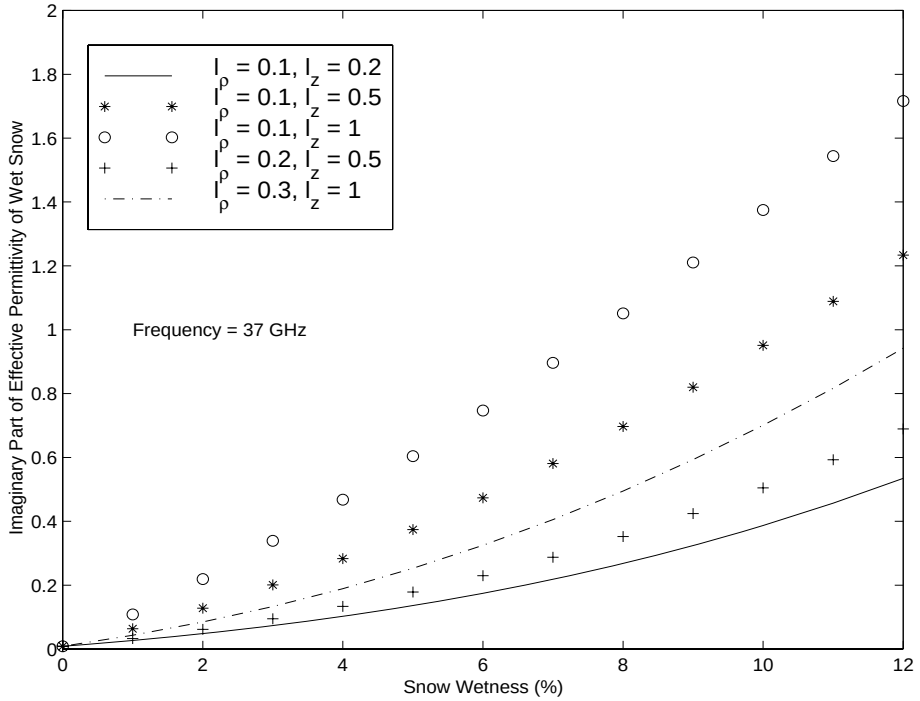


(b)

Figure 4.7 Computed effective permittivity of wet snow at 37 GHz with various correlation lengths (in mm). (a) Real part of the effective permittivity. (b) Imaginary part of the effective permittivity.

The results from the two-phase strong fluctuation theory model with non-symmetrical inclusions are compared with those from the three-phase strong fluctuation theory with symmetrical inclusions, Debye-Like semi-empirical model and the experimental data collected for snow (*Hallikainen et. al 1986*).

In the two-phase strong fluctuation theory model with non-symmetrical inclusions, we used the following values of the correlation lengths of water inclusions in horizontal and vertical directions are $l_\rho$ = 0.11 mm, $l_z$ = 0.43 mm. These values gave the best results in comparison with the experimental data at 6, 18 and 37 GHz. In the three-phase strong fluctuation theory model, the radius of spherical scatterers are $a_1$ = 0.4 mm and $a_2$ = 0.7 mm for water and ice particles, respectively (*Jin and Kong 1984*). The comparisons between the two-phase strong fluctuation theory model with non-symmetrical inclusions and three-phase strong fluctuation theory model with symmetrical inclusions, Debye-Like semi-empirical model and the experimental data given in (*Hallikainen et. al 1986*) at 6, 18 and 37 GHz are depicted in Figures 4.8 to 4.10.

The results show that the two-phase strong fluctuation theory model with non-symmetrical inclusions provides a reasonably good agreement with the experimental data and the other models. When the frequency increases from 6 to 37 GHz the two-phase strong fluctuation theory model with non-symmetrical inclusions gives a better fit with experimental data for the real part of permittivity. However, concerning the imaginary part the prediction from the two-phase model underestimates the imaginary part of permittivity at 6 GHz and overestimates it at 37 GHz. The reason for this could be that the sensitivity of two-phase model to size and shape of water inclusions are different at different frequencies as shown in Figure 4.5, 4.6 and 4.7. Another explanation could be that according to (*Hallikainen et. al 1986*), the water inclusions in wet snow appear needle-like in shape for the volume fraction below $f_v = 3\%$. However, they become disk-like for $f_v \geq 3\%$. This change in shape appears to be due to the transition from the pendular regime to the funicular regime. In [**P4**], we used this approach; we used different correlation lengths at different snow volume fractions and we got good results.

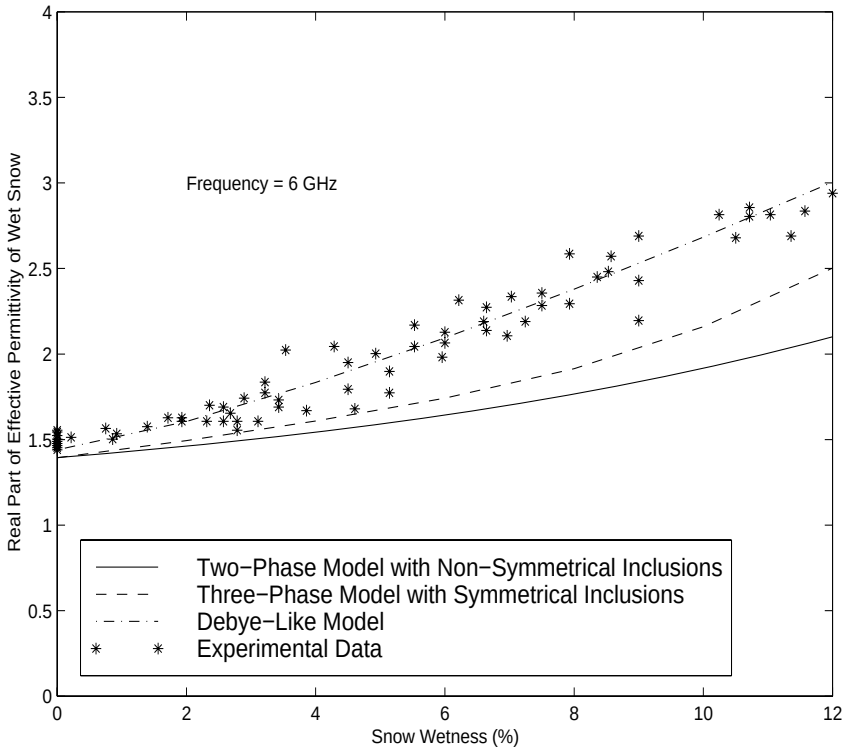


(a)

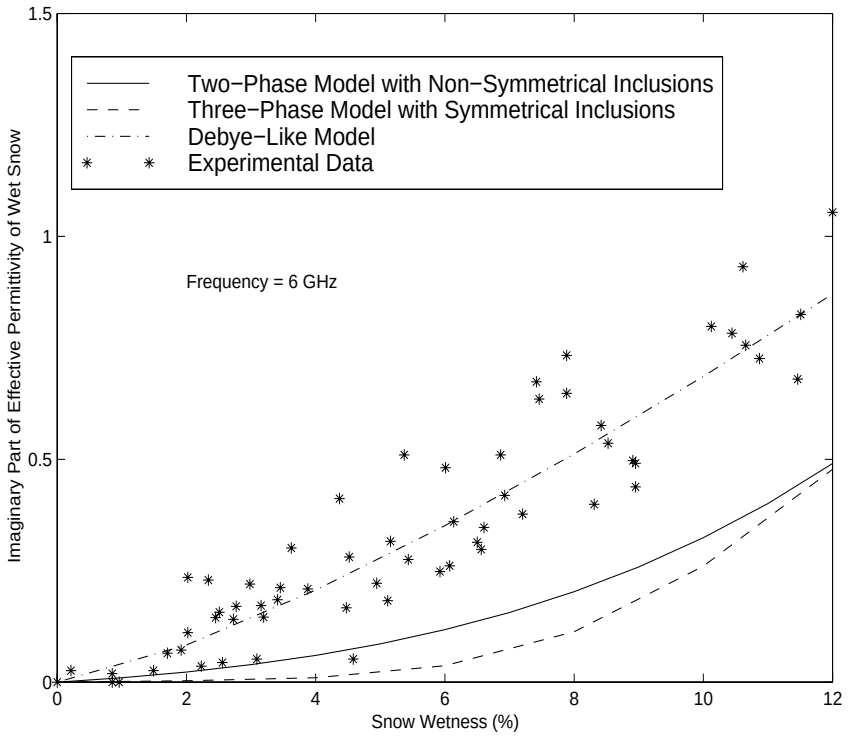


(b)

Figure 4.8 Comparison of two-phase strong fluctuation theory model with experimental data (*Hallikainen et. al 1986*) for the effective permittivity of wet snow and other models at 6 GHz. (a) Real part of the effective permittivity. (b) Imaginary part of the effective permittivity.

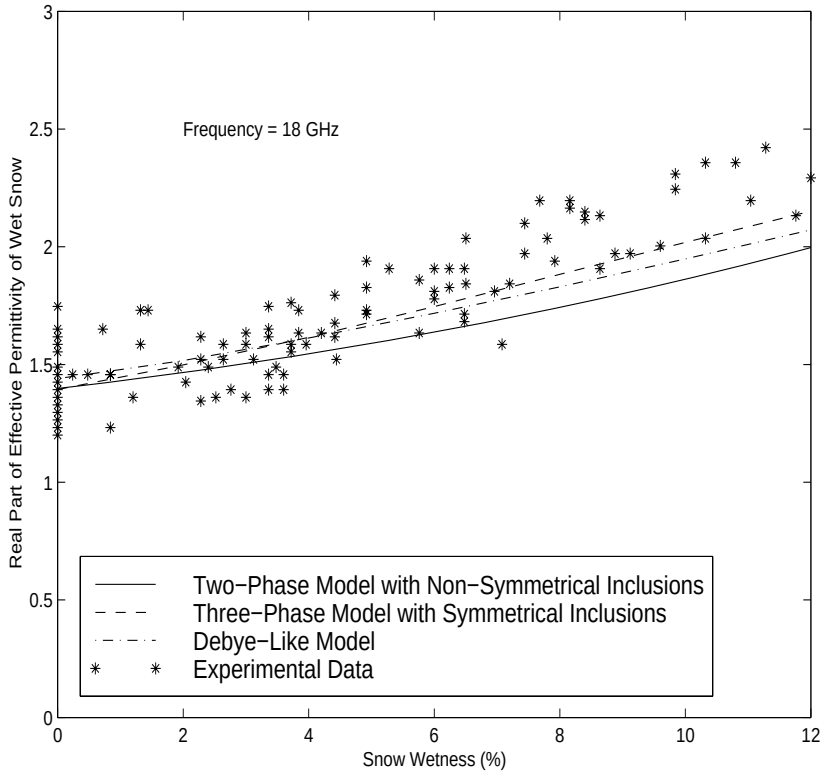


(a)

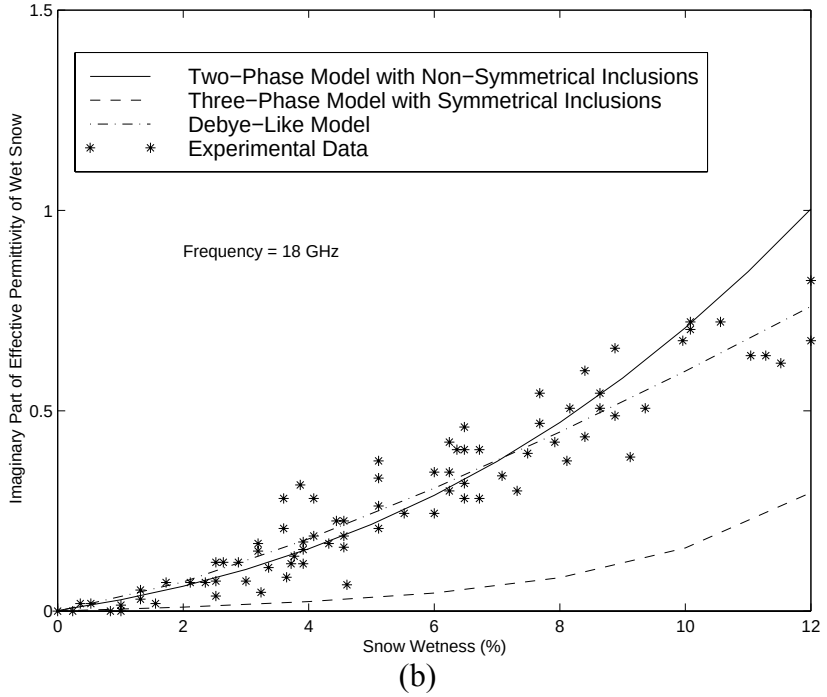


(b)

Figure 4.9 Comparison of two-phase strong fluctuation theory model with experimental data (*Hallikainen et. al 1986*) for the effective permittivity of wet snow and other models at 18 GHz. (a) Real part of the effective permittivity. (b) Imaginary part of the effective permittivity.

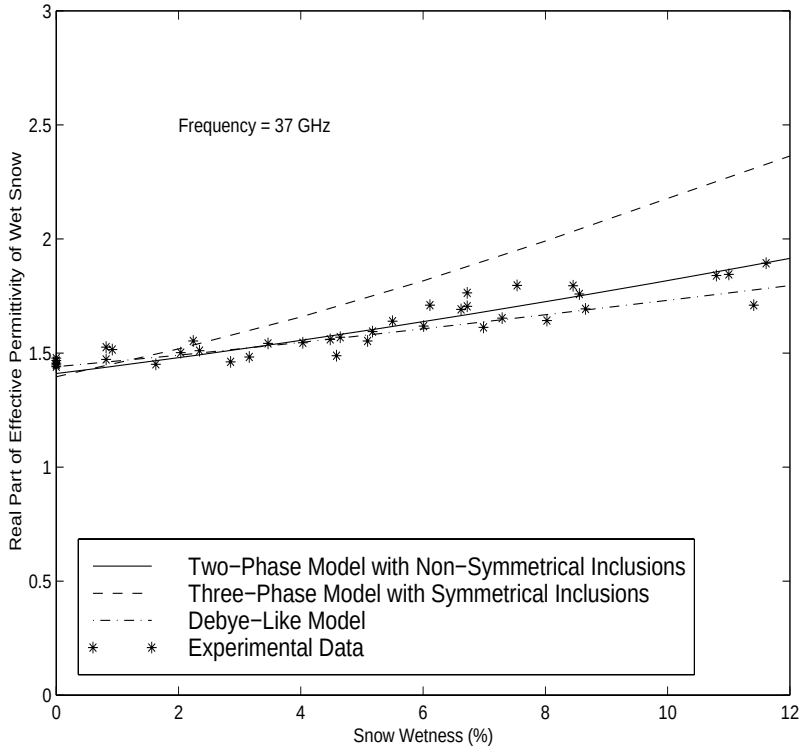


(a)

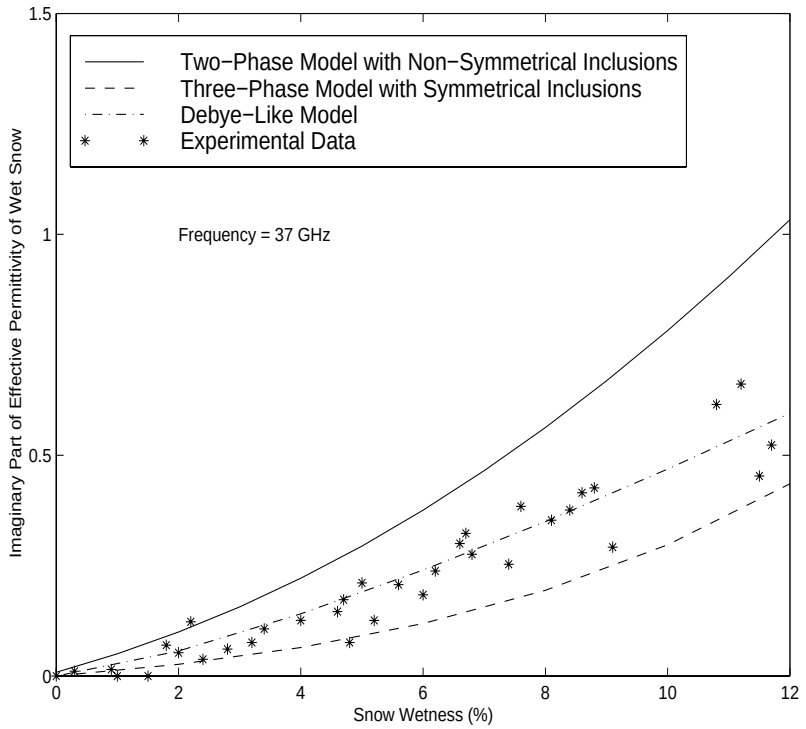


(b)

Figure 4.10 Comparison of two-phase strong fluctuation theory model with experimental data (*Hallikainen et. al 1986*) for the effective permittivity of wet snow and other models at 37 GHz. (a) Real part of the effective permittivity. (b) Imaginary part of the effective permittivity.

### 4.4 Brightness Temperature of Wet Snow-Covered Terrain

In [**P4**], the development of a model is presented to describe microwave emission from wet snow. The model is based on the radiative transfer and the strong fluctuation theory. The effective permittivity is calculated by using the two-phase strong fluctuation theory model with non-symmetrical inclusions [**P3**]. The phase matrix and extinction coefficients of wet snow for an anisotropic correlation function with azimuth symmetric are used. The vector radiative transfer equation for a layer of a random medium was solved by using Gaussian quadrature and Eigen analysis.

Comparisons with brightness temperature data at 11, 21 and 35 GHz (*Wiesmann et.al, 1996*) are shown in Figure 4.11 to 4.13, respectively. In the experimental data (*Wiesmann et.al, 1996*), a set of three microwave radiometers at frequencies 11, 21 and 35 GHz was used to measure the brightness temperatures of melting snow at an Alpine test site, Weissfluhjoch, Davos, Switzerland on June 20, 1995. Only limited ground-truth information is given in (*Wiesmann et.al, 1996*): the snow depth is 81 cm, the air temperature is $8^{o}$ C, the snow temperature is $0.1^{o}$ C at the top of snow layer, and $0^{o}$ C on the ground. In the model, the basic set of input parameters for the calculations is listed in Table 1 and the values the correlation lengths of water inclusions in vertical and horizontal direction $l_{\rho} = 0.11$ mm and $l_{z} = 0.43$ mm. It is shown that the model agrees with the experimental data.

Table 1: The basic set of input parameters

| $f$ (GHz) | $T$ (K) | $H$ (mm) | $f_{v\_ice}$ | $D_{ice}$ (mm) | $f_{v\_water}$ |
|---|---|---|---|---|---|
| 11, 21, 35 | 273 | 810 | 0.3 | 0.8 | 0.05 |

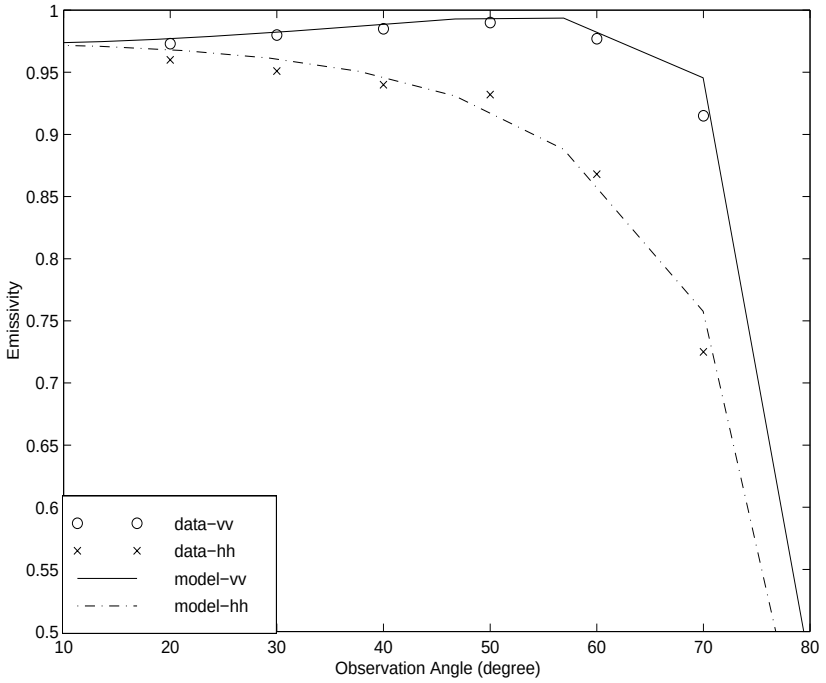


Figure 4.11 Comparison of the predictions from the wet snow model with experimental emissivity values (*Wiesmann et.al, 1996*) at 11 GHz.

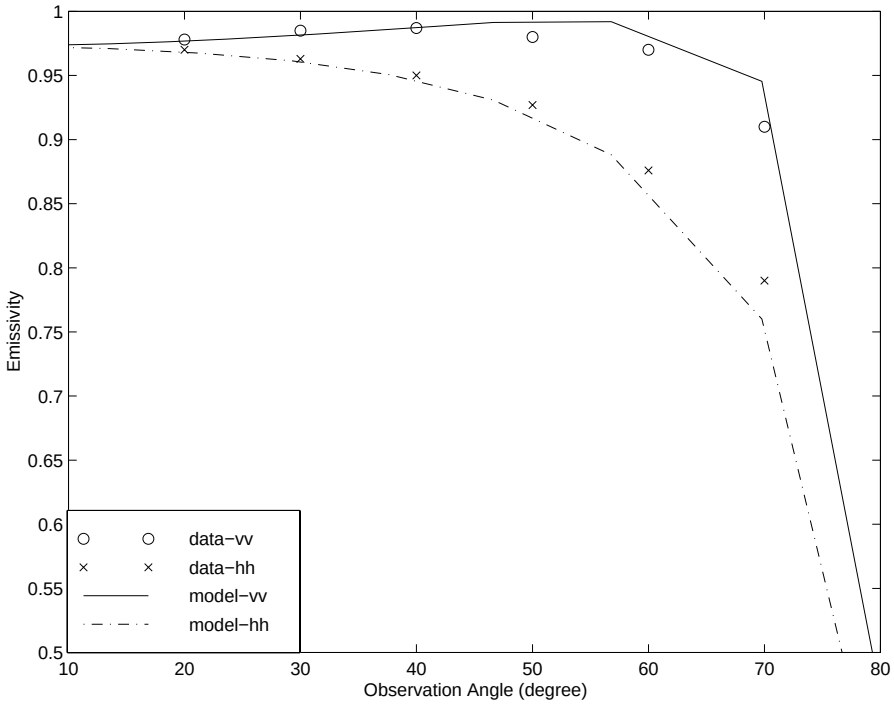


Figure 4.12 Comparison of the predictions from the wet snow model with experimental emissivity values (*Wiesmann et.al, 1996*) at 21 GHz.

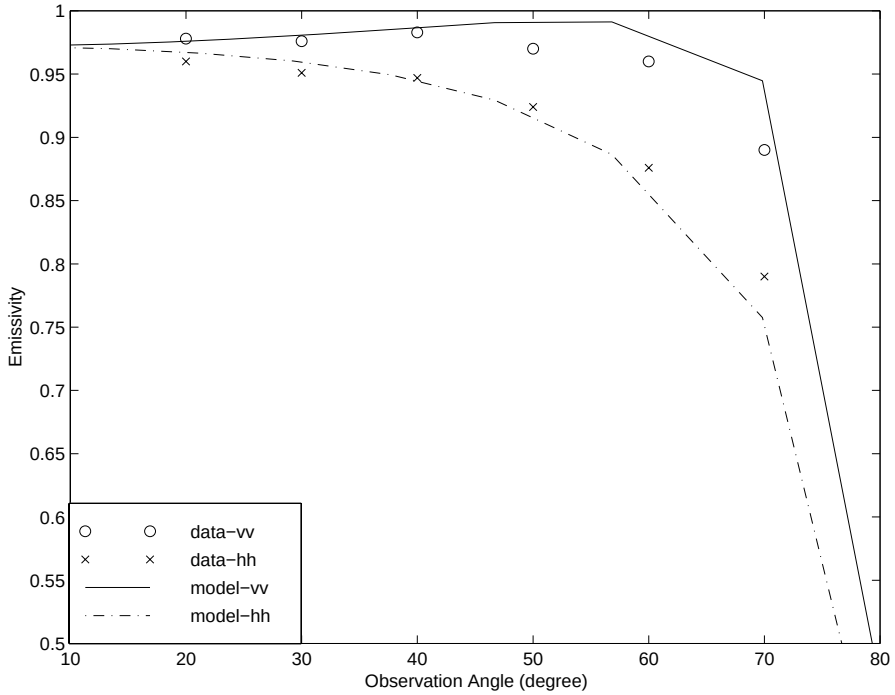


Figure 4.13 Comparison of the predictions from the wet snow model with experimental emissivity values (*Wiesmann et.al, 1996*) at 35 GHz.

### 4.5 Backscattering from Wet Snow

The strong fluctuation theory has been applied to calculate scattering from random medium such as snow and vegetation canopy (*Jin and Kong 1984, Tsang and Kong 1981a, Tsang and Kong 1981b, Tsang et. al 1982*). Random medium is characterized by an effective permittivity that describes propagation and attenuation in the medium. Jin and Kong used the strong fluctuation theory with a three-phase mixture (air, ice and water particles) to calculate the permittivity of wet snow (*Jin and Kong 1984*). In their calculation, the shape of scattering inclusions is considered to be spherical. Our studies in [**P3**] show that the real shape of the scatterers may be important and so should be considered in the calculation of the effective permittivity of wet snow.

In [**P5**], the backscattering coefficients of wet snow are calculated from a half space of wet snow (shown in Figure 4.14) by taking into account of the shape of the scatterers using non-symmetrical inclusions in the strong fluctuation theory.

The wet snow is treated as a two-phase mixture, where the water is considered to be particles as inclusions embedded in a background material of dry snow. The shape of the water inclusions is taken into account by using an anisotropic azimuthally symmetric correlation function (*Jin 1989, Tsang and Kong 1981b*).

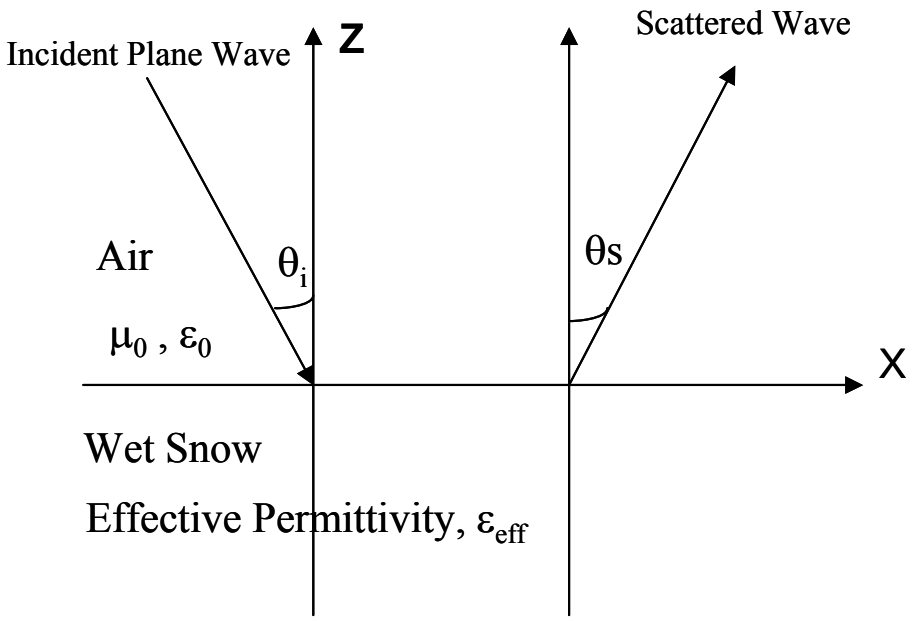


Figure 4.14 Scattering from a half-space wet snow with effective permittivity.

The results of the two-phase strong fluctuation theory model with non-symmetrical inclusions are compared with the three-phase strong fluctuation theory with symmetrical inclusions and the experimental data (*Stiles and Ulaby 1980*) in Figure 4.15. The fractional volumes for water and ice inclusions are 2 and 23 percent, respectively, in both models (*Jin and Kong 1984*). In the two-phase strong fluctuation theory model with non-symmetrical inclusions, the correlation lengths are considered as free fitting parameters. We used the values of the correlation lengths of water inclusions in vertical and horizontal directions which are $l_\rho$ = 0.5 mm, $l_z$ = 0.6 mm. These values are chosen to fit the experimental data (*Jin and Kong 1984*). In the three-phase strong fluctuation theory model, the radii of spherical scatterers are $a_1$ = 0.4 mm and $a_2$ = 0.7 mm

for water and ice particles respectively (*Jin and Kong 1984*). The results are in very good agreement with each other.

We compare the two-phase strong fluctuation theory model with non-symmetrical inclusions with a different set of experimental data (*Stiles and Ulaby 1980*). In (*Stiles and Ulaby 1980*), the experimental data was acquired during February and March 1977 at the test site near Steamboat Springs, Colorado. The temperature of the snowpack varied from –13$^{o}$ C and 0$^{o}$ C. The ground temperature was 0$^{o}$ C, and -1$^{o}$ C. Snow depth, water equivalent and snow wetness were 26 cm, 5.9 cm and 3.1 %, respectively. In Figure 4.15, the backscattering coefficients are plotted as a function of frequency at an incidence angle of 50$^{o}$. In the two-phase strong fluctuation theory model with non-symmetrical inclusions, we used the following values of the correlation lengths of water inclusions in vertical and horizontal directions which are $l_{\rho} = 0.5$ mm, $l_{z} = 0.6$ mm. The fractional volume for water is 3.1 percent which was given in the experimental data (*Stiles and Ulaby 1980*). The comparison shows that the two-phase model with non-symmetrical inclusions provides the good results to the backscattering coefficients of wet snow.

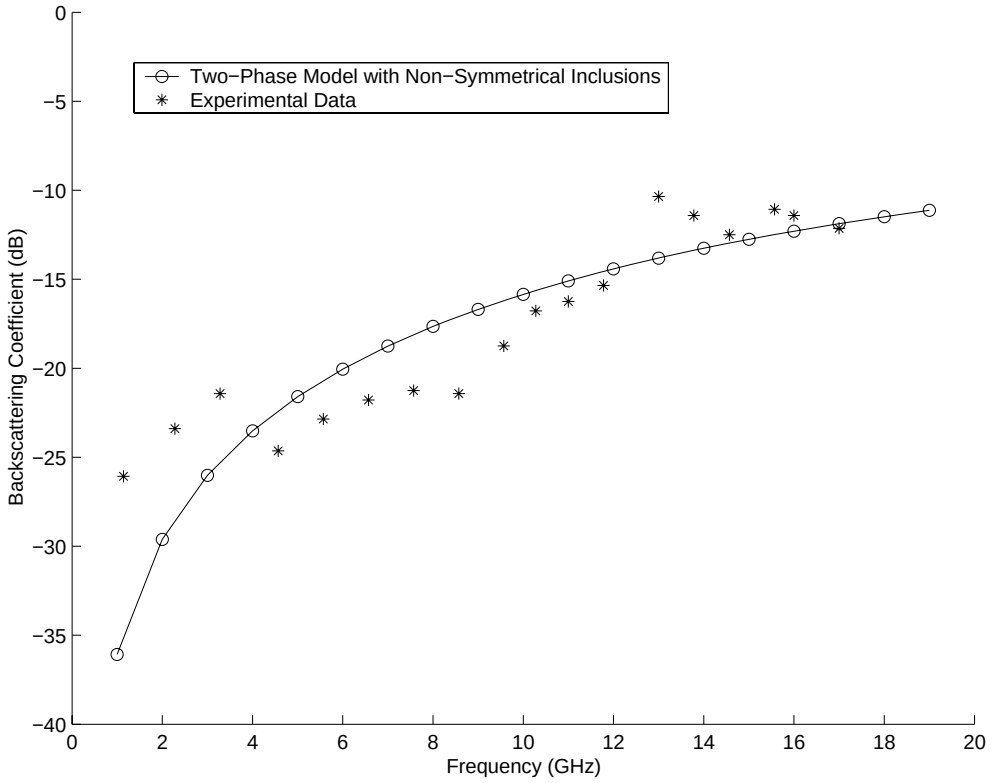


Figuere 4.15 Comparison of two-phase strong fluctuation theory model with non-symmetrical inclusions with experimental data (*Stiles and Ulaby 1980*) for the backscattering coefficients of wet snow as a function of frequency at an incidence angle of $50^{o}$. Snow depth = 26 cm, water equivalent = 5.9 cm, and snow wetness = 3.1 %.

### 4.6 Retrieval of Wet Snow Parameters from Radar Data

We examined in [**P5**] the effect of the size and shape of water inclusions on the backscattering coefficient. In [**P6**], we investigate the relationship between correlation lengths and snow wetness by comparing the results from the two-phase backscattering model with experimental data in (*Stiles and Ulaby 1980*). The effect of size and shape of water inclusions on different snow wetness values was also examined in order to see possible relations between correlation lengths and snow wetness parameters and how these differ at various frequencies. In [**P6**], in order to know what frequencies are high enough to allow comparison between our model (snow contribution only) and data (snow and ground contributions) we estimated the penetration depth versus frequency and snow wetness. The results are in line with previous studies (*Rott et. al, 1992, Mätzler, 2001*).

Figure 4.16 shows a comparison between the two-phase backscattering model with non-symmetrical inclusions and experimental data versus snow wetness for 1.2 GHz, 8.6 GHz, 17 GHz and 35.6 GHz for HH polarization, 50$^o$ angle of incidence, snow depth 45 cm, snow water equivalent 13.5 cm.

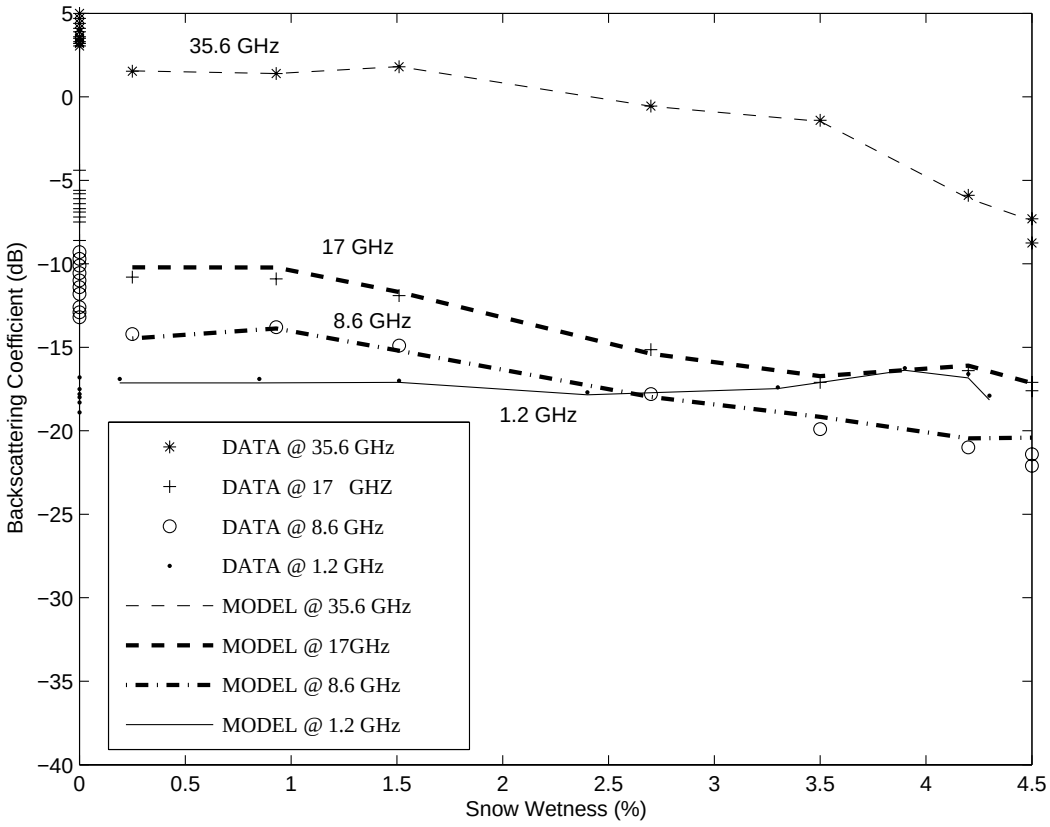


Figure 4.16 Comparison between the two-phase backscattering model with non-symmetrical inclusions and the experimental data (*Stiles and Ulaby 1980*) versus snow wetness at 1.2 GHz, 8.6 GHz, 17 GHz and 35.6 GHz for HH polarization, 50$^o$ angle of incidence, snow depth 45 cm, snow water equivalent 13.5 cm. Different correlation lengths used as a fitting parameter for each frequency [**P6**].

In real life, we need to consider inclusions of the same size and shape at all frequencies. In Figure 4.17, a comparison with experimental data is shown using the same correlation lengths for all frequencies. The backscattering contribution from snow at 1.2 GHz is very low and contribution from ground dominates. The model agrees well with experimental data at 8.6 GHz and 17 GHz, but not at 1.2 GHz and 35.6 GHz. These results are in line with the experimental results (*Stiles and Ulaby 1980*). In (*Stiles and Ulaby 1980*) the snow samples used for wetness

determination were acquired from the top 5cm layer of the snowpack. As explained in more detail in (*Stiles and Ulaby 1980*), the top 5cm layer may be an adequate descriptor of the effective depth at 8.6 GHz and 17 GHz but not at 1.2 GHz and 35.6 GHz. The effective depth is the depth that is responsible for the majority of backscattering contributions. The effective depth at 35.6 GHz may be smaller than 5 cm. On the other hand, the backscattering coefficient at 1.2 GHz is rather independent of snow wetness of the top 5 cm layer due to the greater depth of penetration.

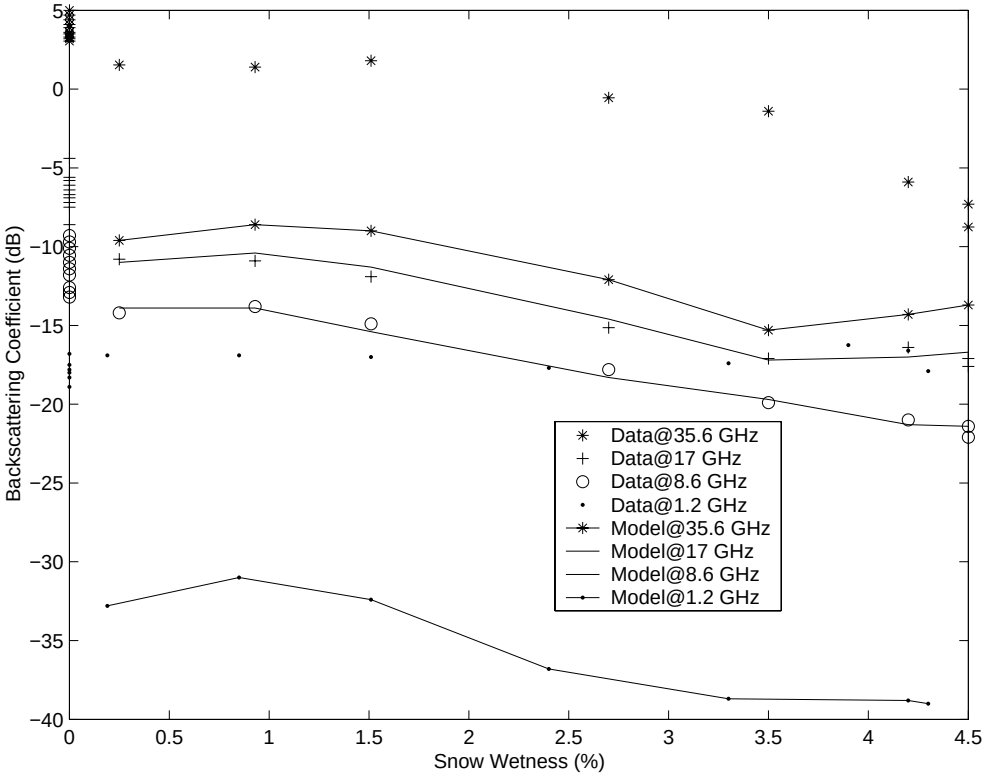


Figure 4.17 The comparison between two-phase backscattering model with non-symmetrical inclusions and the experimental data (*Stiles and Ulaby 1980*) versus snow wetness at 1.2 GHz, 8.6 GHz, 17 GHz and 35.6 GHz for HH polarization, $50^{o}$ angle of incidence, snow depth 45 cm, snow water equivalent 13.5 cm. Same correlation lengths used as a fitting parameter for each frequency [**P6**].

# V Conclusions

The objective of the thesis was to develop microwave models for investigating the complex behaviour of microwave interaction with snow. Papers [**P1**]-[**P2**] combine semi-empirical and empirical models of snow for a forest-snow-ground system. In [**P3**] the two-phase model with non-symmetrical inclusions is presented for calculating the effective permittivity of snow using strong fluctuation theory. Papers [**P4**]-[**P5**] are concerned with developing microwave emission and scattering models for wet snow. Paper [**P6**] investigates the relationship of the physical parameters such as size and shape of inclusions and snow wetness together with the incidence angle and frequency.

The new scientific knowledge achieved in the thesis includes:

- In [**P1**], the radar backscattering signal from dry snow in non-forested (open) areas was examined using polarimetric EMISAR data at L- and C-band. An empirical snow backscatter model at C-band was developed for large, relatively homogeneous areas.
- In [**P2**], the semi-empirical backscattering model approach for a forest-snow-ground system was developed, based on combining the semi-empirical and empirical models developed on the different data sets of passive and active sensors.
- In [**P3**], a model was developed for calculating the effective permittivity of wet snow using the strong fluctuation theory and the results were compared with experimental data. Wet snow was considered as a mixture of dry snow and non-symmetrical water inclusions.
- In [**P4**], a model based on the radiative transfer and the strong fluctuation theory to describe microwave emission from wet snow was developed using the effective permittivity model of wet snow developed in [**P3**].
- In [**P5**], a two-phase backscattering model for wet snow was developed using the effective permittivity model of wet snow developed in [**P3**].

- In [**P6**], the relationship between correlation lengths and snow wetness were presented by comparing results from strong fluctuation theory with the experimental data at 1.2 GHz, 8.6 GHz, 17 GHz and 35.6 GHz. The effects of size and shape of water inclusions at different snow wetness values to backscatter level were shown.

Possibilities to further develop the work in the thesis include:

- The model presented in [**P5**] considers only volume scattering. The two-phase backscattering model needs further developments and should include air-snow and ground-snow interface effects.
- Examining radar backscatter from a half-space of dry snow using the model presented in [**P5**] and verification of the empirical model in [**P1**] to retrieve snow water equivalent parameter.
- Microwave multilayer emission and scattering models of snow.

# VI Summary of Appended Papers

**[P1]**

A statistical analysis for the backscattering coefficient and snow water equivalent was carried out for EMISAR data. EMISAR operates at L-band (1.25 GHz) and C-band (5.3 GHz) and measures at the two frequencies both the amplitude and relative phase of the backscattering coefficient for VV, HH, VH, and HV polarizations. An empirical model is presented to retrieve the snow water equivalent from C-band SAR data for non-forested (open) areas. The model works better to retrieve snow water equivalent for large and relatively homogeneous areas.

**[P2]**

A semi-empirical backscattering model of forest-snow-ground system, which is a function of the forest stem volume, and the snow water equivalent is developed. Applicability of the forest transmissivity formulas developed by using the different data sets of passive and active sensors is investigated.

**[P3]**

The strong fluctuation theory is applied to calculate the effective permittivity of wet snow by a two-phase model with non-symmetrical inclusions. In the two-phase model, wet snow is assumed to consist of dry snow (host) and liquid water (inclusions). Numerical results for the effective permittivity of wet snow are illustrated for random media with isotropic and anisotropic correlation functions. A three-phase strong fluctuation theory model with symmetrical inclusions is also presented for theoretical comparison. In the three-phase model, wet snow is assumed to consist of air (host), ice (inclusions) and water (inclusions) and the shape of the inclusions is spherical. The results are compared with the Debye-like semi-empirical model and a comparison with experimental data at 6, 18 and 37 GHz is also presented. The results indicate that (a) the shape and the size of inclusions are important, and (b) the two-phase model with non-symmetrical inclusions provides good results for the effective permittivity of wet snow.

**[P4]**

This paper is concerned with development of a model to describe microwave emission from wet snow. This model is based on the radiative transfer and the strong fluctuation theory. The wet snow is treated as a mixture of dry snow and water inclusions. The shape of the water inclusions is important. The effective permittivity is calculated by using the two-phase strong fluctuation theory model with non-symmetrical inclusions. The phase matrix and extinction coefficients of wet snow for an anisotropic correlation function with azimuth symmetric are used. The vector radiative transfer equation for a layer of a random medium was solved by using Gaussian quadrature and eigen analysis. Comparisons with brightness temperature data at 11, 21 and 35 GHz are made. It is shown that the model agrees with the experimental data.

**[P5]**

The strong fluctuation theory is applied to calculate the scattering from a half space of wet snow. The first and second moments of the fields are calculated using the bilocal and the distorted Born approximations, and the low frequency limit is taken. The effective permittivity of wet snow is calculated using the two-phase model with non-symmetrical inclusions. Numerical results for the backscattering coefficients of wet snow are illustrated for random media with isotropic and anisotropic correlation functions. The results are in good agreement with the experimental data.

**[P6]**

The relationship between correlation lengths and snow wetness is presented comparing strong fluctuation theory with the experimental data at 1.2 GHz, 8.6 GHz, 17 GHz and 35.6 GHz. The effect of snow wetness on the backscattering coefficient is investigated. Numerical results of comparison between the two-phase backscattering model with non-symmetrical inclusions and the experimental data are illustrated at 1.2 GHz, 8.6 GHz, 17 GHz and 35.6 GHz. The effect of size and shape of water inclusions at different snow wetness values to backscatter level is shown. The comparison of angular response of backscattering coefficient (dB) to wet snow between the model and the experimental data is presented at 2.6 GHz, 8.6 GHz, 17 GHz and 35.6 GHz.

# VII References


Ambach, W., and A. Denoth, " The dielectric behavior of snow : A study versus liquid water content, " presented at *NASA Workshop on Microwave Remote Sensing of Snowpack Properties*, NASA CP2153, Ft. Collins, CO, May 20-22, 1980.

Askne, J., and M. Santoro, "Multitemporal repeat pass SAR interferometry of boreal forests," *IEEE Trans. on Geosci. Remote Sensing*, Vol. 43, No. 6, pp. 1219-1228, 2005.

Bernier, M., and J. P. Fortin , " Potential of ERS-1 SAR Data For Snow Cover Monitoring," *Proceeding of IGARSS'92*, Vol.2, pp. 1664 - 1666, 1992.

Calvet, J-C., J-P.Wigneron, E.Mougin, Y.H.Kerr and J.L.Brito, "Plant water content and temperature of the forest from satellite microwave radiometry," *IEEE Trans. on Geosci. Remote Sensing*, Vol. 32, No. 2, pp. 397 - 408, 1994.

Chang, A. T. C., S. G. Atwater, V. V. Salomonson, J. E. Estes, D. S. Simonett, and M. L. Bryan, "L-band radar sensing of soil moisture," *IEEE Trans. on Geosci. Remote Sensing*, Vol. 18, No. 4, pp. 303-310, 1980.

Chauhan, N. R., R. H. Lang, and K. J. Ranson, "Radar modeling of a boreal forest," *IEEE Trans. on Geosci. Remote Sensing*, Vol. 29, pp. 627-638, 1991.

Chen, K.S., W.D. Wu, L. Tsang and J. Shi, "Emission of rough surfaces calculated by the integral equation method with comparison to three-dimensional moment method simulations," *IEEE Trans. on Geosci. Remote Sensing*, Vol. 41, No. 1, pp. 90 - 101, 2003.

Chuah, Hean-Teik, S. Tjuatja, A.K. Fung, J.W. Bredow, "A phase matrix for a dense discrete random medium: evaluation of volume scattering coefficient," *IEEE Trans. on Geosci. Remote Sensing*, Vol. 34, No. 5, pp. 1137 - 1143, 1996.

Colbeck, S.C., "Liquid Distribution and the dielectric constant of wet snow," presented at *NASA Workshop on Microwave Remote Sensing of Snowpack Properties*, NASA CP2153, Ft. Collins, CO, May 20-22, 1980.

Cumming, W., "The dielectric properties of ice and snow at 3.2 centimetres," *J. Applied Physics*, 23, pp. 768 - 773, 1952.

Debye, P., H.R. Anderson, and H. Brumberger, "Scattering by an inhomogeneous solid II. The correlation function and its application," *J. Applied Physics*, 28, pp. 679 – 683, 1957.

Dobson, M.C., F.T. Ulaby, M. Hallikainen, and M. El-Rayes, " Microwave dielectric behaviour of wet soil-Part II:dielectric mixing models," *IEEE Trans. on Geosci. Remote Sensing*, Vol. 23, No. 1, pp. 35-46, 1985.

Dobson, M. C. and F. T. Ulaby,"Preliminary evaluation of the SIR-B response to soil moisture, surface roughness and crop canopy cover," *IEEE Trans. on Geosci. Remote Sens*ing, Vol. 24, No. 4, pp. 517-526, 1986.

Dobson, M.C., F.T. Ulaby, T. Le Toan, A. Beaudoin, E.S. Kasischke, and N. Christensen, "Dependence of radar backscatter on coniferous biomass," *IEEE Trans. on Geosci. Remote Sens*ing, Vol. 30, No. 2, pp. 412-415, 1992.

Du, J., S. Jiancheng, S. Tjuatja, and K.S. Chen, "A combined method to model microwave scattering from a forest medium," *IEEE Trans. on Geosci. Remote Sensing*, Vol. 44, No. 4, pp. 815 - 824, 2006.

Dubois, P.C., J. J. van Zyl, and E. T. Engman, “Measuring soil moisture with imaging radars,” *IEEE Trans. on Geosci. Remote Sens*ing, 1995.

Durden, S.L., J.J. Van Zyl, and H.A. Zebker, “Modeling and observation of the radar polarization signature of forested areas,” *IEEE Trans. on Geosci. Remote Sensing,* Vol. 27, No. 3, pp. 290-301, 1989.

Fung, A.K., and H.J.Eom, “A study of backscattering and emission from closely packed inhomogeneous media,” *IEEE Trans. on Geosci. Remote Sensing*, Vol. GE-23, No. 5, pp. 761 - 767, 1985.

Fung, A.K., Z. Li, and K.S. Chen, “Backscattering from a randomly rough dielectric surface,” *IEEE Trans. on Geosci. Remote Sensing*, Vol. 30, pp. 356 - 369, 1992.

Fung, A.K., *Microwave Scattering and Emission Models and their Applications*, Artech House, 573 p., 1994.

Fung, A.K., S. Tsuatja, J.W. Bredow, H.T. Chuah, "Dense medium phase and amplitude correction theory for spatially and electrically dense media," *Proceedings of IGARSS’95 Symposium,* Vol. 2 , pp.1336 – 1338, 1995.

Glen, J.W., and P.G. Paren,” The electrical properties of snow and ice,” *J. Glaciol.*, vol. 15, pp. 15-38, 1975.

Hallikainen, M., F. Ulaby, M. Dobson, M. El-Rayes and L. Wu, “Microwave dielectric behaviour of wet soil Part I: empirical equations and experimental observations”, *IEEE Trans. on Geosci. Remote Sensing*, Vol. 23, No. 1, pp. 25 - 34, 1985.

Hallikainen, M., F. Ulaby, and M. Abdelrazik, "Dielectric properties of snow in the 3 to 37 GHz range," *IEEE Trans. on Antennas and Propagation*, Vol. 34, No. 11, pp. 1329 - 1340, 1986.

Hallikainen, M., and P. Jolma, "Comparison of algorithms for retrieval of snow water equivalent from Nimbus-7 SSMR data in Finland," *IEEE Trans. on Geosci. Remote Sensing*, Vol. 30, No.1, pp. 124-131, 1992.

Huining, W., "Microwave emission models of snow," *Doctor of Technology Thesis, Report 46, Laboratory of Space Technology, Helsinki University of Technology*, Espoo, 2001.

Irisov, V.G., "Small-slope expansion for thermal and reflected radiation from a rough surface," *Waves Random Media*, Vol. 7, No. 1, pp. 1-10, 1997.

Izzawati, E.O. Wallington, I.H. Woodhouse, "Forest height retrieval from commercial X-band SAR products," *IEEE Trans. on Geosci. Remote Sensing*, Vol. 44, No. 4, pp. 863 - 870, 2006.

Jackson, T. J., A. Chang, and T. J. Schmugge, "Active microwave measurements for estimating soil moisture in Oklahoma," *Photogram. Eng. Rem. Sens*., Vol. 4, pp. 801-805, 1981.

Jin, Y.Q and J.A. Kong, "Strong fluctuation theory for electromagnetic wave scattering by a layer of random discrete scatters," *J. Applied Physics*, 55, pp. 1364 - 1369, 1984.

Jin, Y.Q., "The radiative transfer equation for strongly-fluctuating continuous random media," *J. Quant. Spectrosc. Radiat. Transfer*. 42: pp. 529 - 537, 1989.

Kendra, J.R., K. Sarabandi, and F.T. Ulaby, “Radar measurements of snow: experiment and analysis,” *IEEE Trans. on Geosci. Remote Sensing*, Vol. 36, No. 4, pp. 864-879, 1998.

Kong, J.A., R. Shin, J. Shiue and L. Tsang, “Theory and experiment for passive microwave remote sensing of snowpacks,” *J. Geophys. Res.*, Vol. 48, No. B10, pp. 5669 - 5673, 1979.

Koskinen, J., J. Pulliainen, and M. Hallikainen , “ The Use of ERS-1 SAR Data in Snow Melt Monitoring, “ *IEEE Trans. on Geosci. Remote Sensing*, Vol. 35, No.3, pp.601-610, 1997.

Koskinen, J., “Snow monitoring using microwave radars,” *Doctor of Technology Thesis, Report 44, Laboratory of Space Technology, Helsinki University of Technology*, Espoo, 2001.

Kruopis, N, J. Praks, A.N. Arslan, H. Alasalmi, J. Koskinen, and M. Hallikainen, "Passive microwave measurements of snow-covered forest areas in EMAC'95," *IEEE Trans. on Geosci. Remote Sensing*, Vol. 37, No. 6, pp. 2699-2705, 1999.

Kurvonen, L., “Radiometer measurements of snow in Sodankylä 1991-93,” *Helsinki University of Technology, Laboratory of Space Technology, Report 16,* 1994.

Le Toan, T., A. Beaudoin, J. Riom, and D. Guyon, “Relating forest biomass to SAR data,” *IEEE Trans. on Geosci. Remote Sens*ing, Vol. 30, No. 2, pp. 403-411, 1992.

Liang, P., M. Moghaddam, L.E. Pierce, and R.M. Lucas, “Radar backscattering model for multilayer mixed-species forest,” *IEEE Trans. on Geosci. Remote Sensing*, Vol. 43, No. 11, pp. 2612-2626, 2005.

Lim H.H., M.E. Veysoglu, S.H. Yueh, R.T. Shin, and J.A. Kong, "Random medium model approach to scattering from a random collection of discrete scatters," *J. Electrom. Waves and Appl.* Vol. 8, pp. 801 - 817, 1994.

Lin D. S., E. F. Wood, K. Beven and S. Saatchi, "Soil moisture estimation over grass-covered areas using AIRSAR," *Int. J. Rem. Sens.*, Vol. 15, No. 11, pp. 2323-2343, 1994(a).

Lin D. S., E. F. Wood, P. Troch, M. Mancini, T. Jackson,"Comparisons of remotely sensed and model-simulated soil moisture over a heterogeneous watershed," *Rem. Sens. Environ.*, Vol. 48, pp 159-171, 1994(b).

Macelloni, G., S. Paloscia, P.Pampaloni, and R. Ruisi "Airborne multifrequency L-to Ka-band radiometric measurements over forests," *IEEE Trans. on Geosci. Remote Sensing*, Vol. 39, No. 11, pp. 2507- 2513, 2001.

Macelloni, G., S. Paloscia, and P.Pampaloni, "Monitoring of melting refreezing cycles of snow with microwave radiometers: The microwave Alpine snow melting experiment (MASMEx 2002-2003)," *IEEE Trans. on Geosci. Remote Sensing*, Vol. 43, No. 11, pp. 2431- 2442, 2005.

Malnes, E. et al., "Development of generic earth observation based snow parameter retrieval algorithms**,"** EnviSnow final report, Contract nr. EVG1-CT-2001-00052, September 20, 2005.

Markus, T., D.C. Powell, J.R. Wang, "Sensitivity of passive microwave snow depth retrievals to weather effects and snow evoluation," *IEEE Trans. on Geosci. Remote Sensing*, Vol. 44, No. 1, pp. 68 - 77, 2006.

McDonald, K. C. and F. T. Ulaby, "Radiative transfer modeling of discontinuous tree canopies at microwave frequencies," *Int. J. Rem. Sens*., Vol. 14, No. 11, pp. 2097-2128, 1993.

Mätzler, C., and E. Schanda, “Snow mapping with active microwave sensors,” *International Journal of Remote Sensing*, Vol. 15, No. 2, pp. 409-422, 1983.

Mätzler, C., H. Aebischer, and E. Schanda, ”Microwave dielectric properties of surface snow,” *IEEE J. Oceanic Eng.*, Vol. OE-9, pp. 366-371, 1984.

Mätzler, C., and U. Wegmüller, “Dielectric properties of fresh-water ice at microwave frequencies,” *J. Phys. D: Appl. Phys. 20*, pp. 1623 - 1630, 1987.

Mätzler, C., “Passive microwave signatures of landscapes in winter,” *Meteorology and Atmospheric Physics,* Vol. 54, pp. 241-260, 1994.

Mätzler C., “Autocorrelation functions of granular media with free arrangement of spheres, spherical shells or ellipsoids,” *J. Applied Physics*, Vol. 81, pp. 1509 - 1517, 1997.

Mätzler, C., “Applications of SMOS over terrestrial ice and snow,” SMOS Workshop, DLR, Oberpfaffenhofen, Germany, December 10-12, 2001.

Nghiem, S. V., R. Kwok, J. A. Kong and R. T. Shin, “A model with ellipsoidal scatterers for polarimetric remote sensing of anisotropic layered media,” *Radio Sci*., Vol. 28, pp. 687 - 703, 1993.

Nghiem, S. V., R. Kwok, S. H. Yueh, J. A. Kong, C. C. Hsu, M. A. Tassoudji and R. T. Shin, “Polarimetric scattering from layered media with multiple species of scatterers,” *Radio Sci*., Vol. 30, pp. 835 - 852, 1995.

Nghiem, S. V., R. Kwok, J. A. Kong, R. T. Shin, S. A. Arcone and A. J. Gow, “An electrotheromdynamic model with distributed properties for effective permittivity of sea ice,” *Radio Sci*., Vol. 31, pp. 297 - 311, 1996.

Nolan, M., and D.R. Fatland, “Penetration depth as DInSAR observable and proxy for soil moisture,” *IEEE Trans. on Geosci. Remote Sensing*, Vol. 41, No. 3, pp. 532 - 537, 2003.

Oh, Y., K. Sarabandi, and F. T. Ulaby, “An empirical model and an inversion technique for radar scattering from bare soil surfaces,” *IEEE Trans. on Geosci. Remote Sensing*, Vol. 30, No. 2, pp. 370-381, 1992.

Peplinski, N., F.T. Ulaby, and M.C. Dobson, “Dielectric properties of soil in the 0.3 – 1.3 GHz range,” *IEEE Trans. on Geosci. Remote Sens*ing, Vol. 33, pp. 803-807, 1995.

Peplinski, N., F.T. Ulaby, and M.C. Dobson, “Correction to dielectric properties of soil in the 0.3 – 1.3 GHz range,” *IEEE Trans. on Geosci. Remote Sens*ing, Vol. 33, pp. 1340, 1995.

Pulliainen, P., “Investigation on the backscattering properties of Finnish boreal forests at C- and X-Band: Semi-empirical modeling approach,”*Doctor of Technology Thesis, Report 19, Laboratory of Space Technology, Helsinki University of Technology*, Espoo, 119 p., 1994.

Pulliainen, J., K. Heiska, J. Hyyppä, and M. Hallikainen, “Backscattering properties of boreal forests at C- and X-band,” *IEEE Trans. on Geosci. Remote Sens*ing, Vol. 32, No. 5, pp. 1041-1050, 1994.

Pulliainen, J., P.Mikkelä, and M.Hallikainen, "Seasonal dynamics of C-band backscatter of boreal forests with applications to biomass and soil moisture estimation," *IEEE Trans. on Geosci. Remote Sensing*, Vol. 34, pp. 758-770, 1996.

Pulliainen, J., L.Kurvonen, and M.Hallikainen, " Multi-temporal behavior of L- and C-band SAR observations of boreal forest," *IEEE Trans. on Geosci. Remote Sensing*, Vol. 37, pp. 927-937, 1999.

Richards, J. A., G-Q. Sun, and D. S. Simonett, “L-band radar backscatter modeling of forest stands,” *IEEE Trans. on Geosci. Remote Sens*ing, Vol. 25, pp. 487-498, 1987.

Ridley, J. K., “Snow properties from passive microwave observations of Antarctica.” *Proceedings of IGARSS’91 Symposium,* pp. 2329 - 2332, 1991.

Rott, H., C.Mätzler, D.Strobl, S.Bruzzi, and K.G., Lenhart, “Study on SAR land applications for snow and glacier monitoring,” *Institut für Meteorologie und Geophysik Universität Innsbruck, European Space Agency Contract, Final Report*, 1988.

Rott, H., R.E.Davis, and J.Dozier, “Polarimetric and multifrequency SAR signatures of wet snow,” *Proceedings of IGARSS’92 Symposium*, Vol. 2, pp.1658 – 1660, 1992.

Shi, J., and J. Dozier, "Measurement of snow and glacier covered areas by single-polarization SAR", *Annals of Glaciology*, pp. 72-76, vol. 17, 1993.

Shi, J., and J. Dozier, "Inferring snow wetness using SIR-C C-band polarimetric synthetic aperture radar", *IEEE Trans. on Geosci. Remote Sensing*, Vol. 33, No. 4, pp. 905-914, 1995.

Shi, J., and J. Dozier, “Estimation of snow water equivalence using SIR-C/X-SAR,” *Proceedings of IGARSS’96*, Vol. 4, pp. 2002-2004, 1996.

Shi, J., and J. Dozier, “Estimation of snow water equivalence using SIR-C/X-SAR, Part I: Inferring snow density and subsurface properties,” *IEEE Trans. on Geosci. Remote Sens*ing, Vol. 38, No. 6, pp. 2465-2474, 2000.

Shi, J., and J. Dozier, “Estimation of snow water equivalence Using SIR-C/X-SAR, Part II: Inferring snow depth and particle size,” *IEEE Trans. on Geosci. Remote Sensing*, Vol. 38, No. 6, pp. 2475-2488, 2000.

Sihvola, A.H., *Electromagnetic Mixing Formulas and Applications*, IEE Electromagnetic Wave Series 47, 1999.

Stiles, W.H. and F.T.Ulaby, " The active and passive microwave response to snow parameters 1. Wetness," *Journal of Geophysical Research,* vol. 85, no. c2, pp. 1037-1044, 1980.

Stogryn, A., “Strong fluctuation theory for moist granular media,” *IEEE Trans. on Geosci. Remote Sensing*, Vol. 23, pp. 78 - 83, 1985.

Stogryn, A., “A study of the microwave brightness temperature of snow from the point of view of strong fluctuation theory,” *IEEE Trans. on Geosci. Remote Sensing*, Vol. 24, No. 2, pp. 220 -231, 1986.

Sun, G., D. S. Simonett, and A. H. Strahler, “A radar backscatter model for discontinuous forest canopies,” *IEEE Trans. on Geosci. Remote Sens*ing, Vol. 29, pp. 639-650, 1991.

Tikhonov, V. V., “Model of complex dielectric constant of wet and frozen soil in the 1-40 GHz frequency range,” *Proceedings of IGARSS´94 Symposium*, Vol. 3, pp. 1576-1578, 1994.

Tiuri, M.E., A. Sihvola, E.G. Nyfors and M.T. Hallikainen, “The complex dielectric constant of snow at microwave frequencies,” *IEEE J. Oceanic Eng.*, Vol. 9, pp. 377 - 382, 1984.

Tjuatja, S., A.K. Fung, and J.W. Bredow, "A scattering model for snow-covered sea ice," *IEEE Trans. on Geosci. Remote Sensing*, Vol. 30, No. 4, pp. 804 - 810, 1992.

Tjuatja, S., A.K. Fung, and M.K. Dawson, "An analysis of scattering and emission from sea ice," *Remote Sensing Reviews*, Vol. 7, pp. 83 - 106, 1993.

Tjuatja, S., A. K. Fung, J. C. Comiso, "Scattering and emission from dry snow in the range 35 -140 GHz," *Proceedings of IGARSS'96 Symposium,* pp. 2008 - 2010, 1996.

Tsang L., and J.A. Kong, "The brightness temperature of a half-space random medium with nonuniform temperature profile," *Radio Sci*., Vol. 10, pp. 1025 - 1033, 1975.

Tsang L., and J.A. Kong, "Thermal microwave emission from half-space random media," *Radio Sci*., Vol. 11, pp. 599 - 609, 1976.

Tsang L., and J.A. Kong, "Thermal microwave emission from a three-layer random medium with three-dimensional variations," *IEEE Trans. on Geosci. Remote Sensing*, Vol. 18, No. 2, pp. 212 - 216, 1980a.

Tsang L., and J.A. Kong, "Multiple scattering of electromagnetic waves by random distribution of scatterers with coherent potential and quantum mechanical formalism," *J. Applied Physics,* Vol. 15, pp. 3465-3485, 1980b.

Tsang L., and J.A. Kong, "Application of strong fluctuation random medium theory to scattering from vegetation-like half space," *IEEE Trans. on Geosci. Remote Sensing*, Vol. 19, No. 1, pp. 62 - 69, 1981(a).

Tsang L., and J. A. Kong, "Scattering of electromagnetic waves for random media with strong permittivity fluctuations," *Radio Sci*., Vol. 16, pp. 303 - 320, 1981(b).

Tsang, L., J. A. Kong and R. W. Newton, "Application of strong fluctuation random medium theory to scattering of electromagnetic waves from a half-space of dielectric mixture," *IEEE Trans. on Antennas and Propagation,* Vol. 30, No. 2, pp. 292 - 302, 1982.

Tsang, L., J. A. Kong and R. T. Shin, *Theory of Microwave Remote Sensing*, Wiley Series in Remote Sensing, J. A. Kong (ed.), New York. 1985.

Tsang, L., and A. Ishimaru, "Radiative wave equation for vector electromagnetic propogation in dense nontenuous media," *J.Electrom. Waves and Appl.,* Vol. 1, pp. 52-72, 1987.

Tsang, L., "Passive remote sensing of dense nontenous media," *J. Electrom. Waves and Appl.* Vol. 1, pp. 159 - 173, 1987.

Tsang, L., Zhengxiao Chen, Seho Oh, Robert J. Marks II, A. T. C. Chang, "Inversion of snow parameters from passive microwave remote sensing measurements by a neuarl network trained with a multiple scattering model," *IEEE Trans. on Geosci. Remote Sensing*, Vol. 30, No. 5, pp. 1015 - 1024, 1992.

Tsang, L., K.H. Ding, S.E Shih, "Monte Carlo simulations of scattering of electromagnetic waves from dense distributions of nonspherical particles," *Proceedings of IGARSS'97 Symposium*, Vol. 2 , pp. 919 - 921, 1997.

Tsang, L., and J.A. Kong, *Scattering of Electromagnetics Waves: Advanced Topics,* New York: Wiley, 2001.

Tsang, L., J.A.Kong, K.H.Ding, and C.O. Ao, *Scattering of Electromagnetic Waves: Numerical Simulations*, New York: Wiley Interscience, 2001.

Tsang, L., K. Ding, and A.T.C., Chang, "Scattering by densely packed sticky particles with size distributions and applications to microwave emission and scattering from snow," *Proceedings of IGARSS'2003 Symposium,* pp. 2844 - 2846, 2003.

Ulaby, F. T and P. P. Batlivala, "Optimum radar parameters for mapping soil moisture," *IEEE Trans. on Geosci. Electron.*, Vol. 14, No. 2, pp. 81-93, 1976.

Ulaby, F. T., P. P. Batlivala, and M. C. Dobson, "Microwave backscatter dependence on surface roughness, soil moisture and soil texture: Part I--bare soil," *IEEE Trans. on Geosci. Electron*., Vol. 16, pp. 286-295, 1978.

Ulaby, F.T., and W.H. Stiles," The Active and Passive Microwave Response to Snow Parameters, 1, Water Equivalent of Dry Snow,"*J.Geophys. Res*., Vol. 85, pp. 1045-1049, 1980.

Ulaby F.T., Moore R., Fung A., *Microwave Remote Sensing ,* Vol. I Artech House, Inc., Norwood, MA02062. 1981.

Ulaby F.T., Moore R., Fung A., *Microwave Remote Sensing,* Vol. II Artech House, Inc., Norwood, MA02062, 1982.

Ulaby F.T., Moore R., Fung A., *Microwave Remote Sensing,* Vol.III Artech House, Inc., Norwood, MA02062, 1986.

Ulaby, F. T., K. Sarabandi, K. McDonald, M. Whitt, and M. C. Dobson, "Michigan microwave canopy scattering model," *Int. J. Rem. Sens*., Vol. 11, pp. 1223-1253, 1990.

Ustin, S., *Remote Sensing for Natural Resource Management and Environmental Monitoring,* Manual of Remote Sensing, Vol. 4, p. 768, ISBN: 0-471-31793-4, 2004.

Vallese, F. and J.A. Kong, “Correlation function studies for snow and ice,” *J. Applied Physics*, 52, pp. 4921 - 4925, 1981.

Voronovich, A.G., “Small-slope approximation for electromagnetic waves scattering at a rough interface of two dielectric half-space,” *Waves Random Media,* Vol. 4, No. 3, pp. 337-367, 1994.

Wang, J. R., E. T. Engman, J. C. Shiue, M. Rusek, C. Steinmeier, “The SIR-B observations of microwave backscatter dependence on soil moisture, surface roughness and vegetation covers,” *IEEE Trans. on Geosci. Remote Sensing*, Vol. 24, No. 4, pp. 510-516, 1986.

Weise, T., “Radiometric and structural measurements of snow,” *Ph.D. Thesis*, Institute of Applied Physics, University of Bern, CH-3012 Bern, 1996.

Wen, B.H., L. Tsang, D.P. Winebrenner, and A. Ishimaru, “Dense medium radiative transfer theory: Comparison with experiment and application to microwave remote sensing and polarimetry,”*IEEE Trans. on Geosci. Remote Sensing*, Vol. 28, No. 1, pp. 46 - 59, 1990.

West, R., L. Tsang, D.P. Winebrenner, "Dense medium radiative transfer theory for two scattering layers with a Rayleigh distribution of particle sizes," *IEEE Trans. on Geosci. Remote Sensing*, Vol. 31, No. 2, pp. 426 –437, 1993.

Wiesmann A., T. Strozzi, and T. Weise, “Passive microwave signature catalogue of snow covers at 11, 21, 35, 48 and 94 GHz”, IAP Research Report, No. 96-8, University of Bern, Switzerland, 1996.

Wiesman, A., C. Mätzler, and T. Weise, “Radiometric and structural measurements of snow samples,” *Radio Science,* Vol. 33, pp. 272-289, 1998.

Wiesman, A., and C. Mätzler, “Microwave emission model of layered snowpacks,” *Remote Sens. Environ.,* Vol. 70, pp. 307-316, 1999.

Wigneron, J-P., Y.H. Kerr, A. Chanzy and Y.Q. Jin, “Inversion of surface parameter from passive microwave measurement over a soybean field,” *Remote Sens. Environ*., Vol. 46 pp. 61 - 72,1993 .

Wigneron, J-P., J-C.Calvet, A. Chanzy, O. Grosjean, and L. Laguerre, “A composite discrete-continuous approach to model the microwave emission of vegetation,” *IEEE Trans. on Geosci. Remote Sensing*, Vol. 33, No. 1, pp. 201 - 211, 1995.

Wu, T.D., K.S. Chen, J.Shi and A.K.Fung, “ A transition model for the reflection coefficient in surface scattering,” *IEEE Trans. on Geosci. Remote Sensing*, Vol. 39, No. 1, pp. 2040 - 2050, 2001.

Yueh, S.H., and J.A. Kong, “Scattering from random oriented scatters with strong permittivity Fluctuations,” *J. Electrom. Waves and Appl.* Vol. 4, pp. 983 - 1004, 1990.